SOME INTERFACIAL STUDIES RELATED TO THE RECOVERY OF MINERAL SLIMES IN WATER-ORGANIC LIQUID-SURFACTANT SYSTEM

By

A V FRANCIS
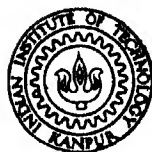
DEPARTMENT OF METALLURGICAL ENGINEERING

INDIAN INSTITUTE OF TECHNOLOGY KANPUR
AUGUST, 1975

SOME INTERFACIAL STUDIES RELATED TO THE RECOVERY OF MINERAL SLIMES IN WATER-ORGANIC LIQUID-SURFACTANT SYSTEM

A Thesis Submitted
In partial Fulfilment of the Requirements
for the Degree of
MASTER OF TECHNOLOGY

By
A V FRANCIS

to the

DEPARTMENT OF METALLURGICAL ENGINEERING

INDIAN INSTITUTE OF TECHNOLOGY KANPUR
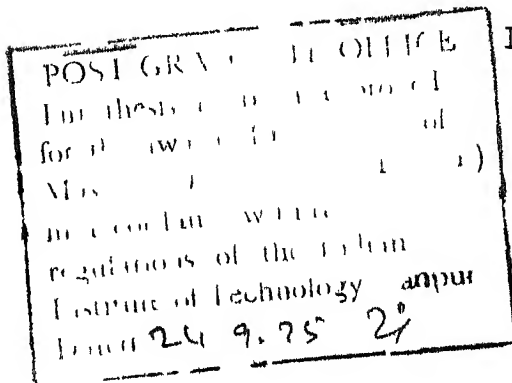AUGUST, 1975

ME-1975-M-FRA-SOM

"

CERTIFICATE

Certified that the work 'Some Interfacial Studies Related to the Recovery of Mineral Slimes in Water-Organic Liquid-Surfactant System' has been carried out under my supervision and the same has not been submitted elsewhere for a degree.

A K Biswas
(A.K. BISWAS)
Professor
Department of Metallurgical Engineering
Indian Institute of Technology
Kanpur.

ACKNOWLEDGEMENTS

CONTENTS

FIGURES

SYNOPSIS

Fine particles of Al_2O_3, Fe_2O_3 and TiO_2 are recoverable in water-kerosene interface in presence of a surfactant such as sodium myristate. The magnitude of recovery depends upon size and surface preparation of the particles as well as the extent of hydrophobization of the solid surface and stability of emulsion. The last two factors depend upon surfactant concentration and pH.

Unsuccessful attempts have been made to correlate magnitudes of adsorption at different interfaces, interfacial tensions and contact angle through the Gibbs Adsorption Equation and Young's Equation. Various reasons have been ascribed to explain the lack of good correlation.

We have observed two phenomena which are not taken into account in Gibbs Adsorption and Young's equation Firstly, after the three phase contact is established, the adsorption at the solid-organic liquid interface is found to be much more than the equilibrium values predicted from two-phase adsorption studies. This excess is evidently due to the transfer of surfactant from the O/W interface on to S/O interface. The second phenomenon relates to heightened adsorption at the three-phase interline. More fundamental work is necessary towards a quantitative understanding of the interfacial recovery processes.

CHAPTER 1

INTRODUCTION

Recovery of mineral slimes (all particles below 10 microns and most below 1 micron) through conventional froth flotation process is a difficult proposition. This accounts for loss of large amounts of valuable slimes in flotation tailings. Several techniques which have been attempted for _preferential_ recovery of certain minerals from slimes are: 1) liquid-liquid extraction process, 2) ultra-flotation/piggy back flotation, 3) selective flocculation, 4) spherical agglomeration, 5) column flotation, 6) electrostatic separation etc. This thesis deals with the fundamental aspect of the first process.

In conventional froth flotation process, mineral particles are rendered hydrophobic by the use of surface-active collector molecules, and gas (usually air) is used as the buoyant medium. This process is less than a century old whereas the usage of oil instead of gas for recovery of mineral particles in the water-oil interface is of more ancient tradition[1,2].

The practice of using oil and obtaining emulsion for collecting mineral particles at the emulsion interface has been recently revived. McCarroll reported

emulsion flotation of manganese ores[3]. Piggy-back flotation of a high proportion of anatase slime on 60 μm calcite carrier particles could be enhanced through use of fatty acid collector and large quantity of light hydrocarbon oil[4].

Various workers demonstrated the role of fine particles in stabilising large interfaces[5-8]. Pickering was the first to show that solid powders can stabilise oil-water dispersions[5]. Hildebrand proposed[6] that a thin layer of the outer liquid is much better protected against rupture if the solid particles project chiefly into the interior of the film. Schulman and Leja[7] as well as Grigorov et al[8] emphasized the role of fine size of particles and large contact angle in stabilising emulsions.

A detailed study[9] of the extraction of fine alumina particles considered a system consisting of particles, alkyl sulphonates of different chain lengths and iso-octane. Greater chain length and aqueous concentration of surfactants yielded greater adsorption from the aqueous phase, contact angle and recovery. Highest extraction occurred when the contact angle exceeded $90°$ and the electrokinetic potential was zero. Recently, Zambrana and co-workers have worked[10] on the recovery of minus 10 micron particles of cassiterite using Aeroson 22 collector and gasoline. Selective recovery of cassiterite has been reported. Various

factors such as collector concentration, pH, agitation speed and oil to water ratio were studied.

Shergold and Mellgren have published the most important series of papers[11-14] on the subject. They have worked on interfacial concentration of minerals in the water-iso-octane interface viz., hematite with sodium dodecyl sulphate as the collector[12a], quartz with dodecyl-amine as the collector[13] and hematite with dodecylamine as the collector[14a]. Various physical factors such as oil to water ratio, degree of agitation and chemical factors such as surfactant concentration, pH etc. were studied. The authors claimed good correlation between mineral recovery at the interface and adsorption on the solid-water interface (Γ_W), contact angle (θ), Zeta potential and work of adhesion [$W_a = \gamma_W(1 - Cos\theta)$] etc. When pH was studied as a variable, maximum recoveries occurred at intermediate pH values where θ and Γ also showed maxima and Zeta potential was very close to zero. The authors recognised the role of surfactant adsorption on the hydrocarbon-solid interface and yet did not undertake any measurement work in this regard. This aspect has been ignored by other workers also.

The present series of investigation has been undertaken to study·

(1) recoverability of rutile slimes in water-hydrocarbon-fatty acid salt systems (recovery of titanium dioxide

slime from paper and pigment industry waste effluents by coagulation/flotation technique has been recently investigated[15]) and also of fine particles of Al_2O_3 and Fe_2O_3 in similar systems, and to study,

(2) the fundamental aspects of liquid-liquid extraction of fine particles (such as mentioned above) — specially the adsorption phenomenon on the hydrocarbon-solid interface and on the three-phase interline which has been hitherto ignored. Some preliminary work on the fundamental aspects was done by A. Bhargava[16] in this laboratory. The present work may be deemed to be an extension of Bhargava's thesis.

CHAPTER 2

MATERIALS

The details of the chemicals and the materials used are mentioned below.

2.1 Oxide Powders

Titanium dioxide powder manufactured by May and Baker Ltd., U.K. was used for liquid-liquid extraction experiments. The estimated purity is greater than 98 per cent and the sample does not contain more than 0.5 per cent water-soluble substance. Sizes of the particles range from $\frac{1}{2}$ to 3 micron.[⊕] The detailed information is given in Fig. 1 and Table 1.

99 per cent pure Aluminum oxide was of B.D.H. (U.K.) variety. Fig. 1 and Table 2 contain the size distribution data for the $\frac{1}{2}$ - 9 μ Al_2O_3 particles. Specific surface area of this sample is 3×10^3 cm^2/g. For certain experiments, coarser variety of Al_2O_3 was also used. Data for coarse Al_2O_3 are given in Fig. 2.

Analytically pure (+99%) Fe_2O_3 powders were used. This had size range between $\frac{1}{2}$ to 4 μ (vide Table 3, Fig. 1). Specific surface area of this sample is 10^4 cm^2/g.

[⊕]The particle size is determined by observing 3 slides of each sample under microscope and each case nearly 600 particles are observed. These observations were giving agreeable results.
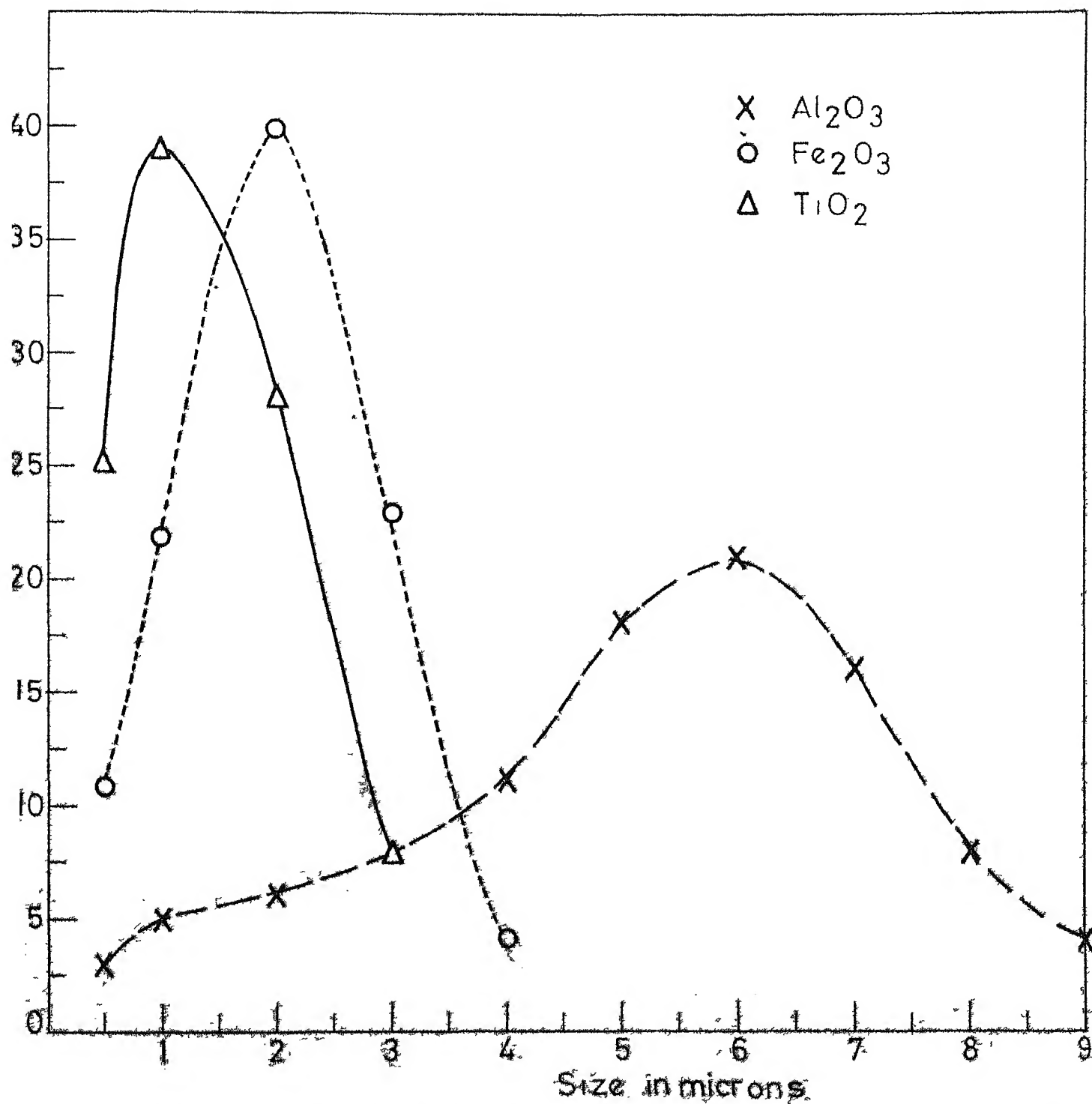
PARTICLE SIZE DISTRIBUTION OF Al_2O_3(Fine),Fe_2O_3 AND TiO
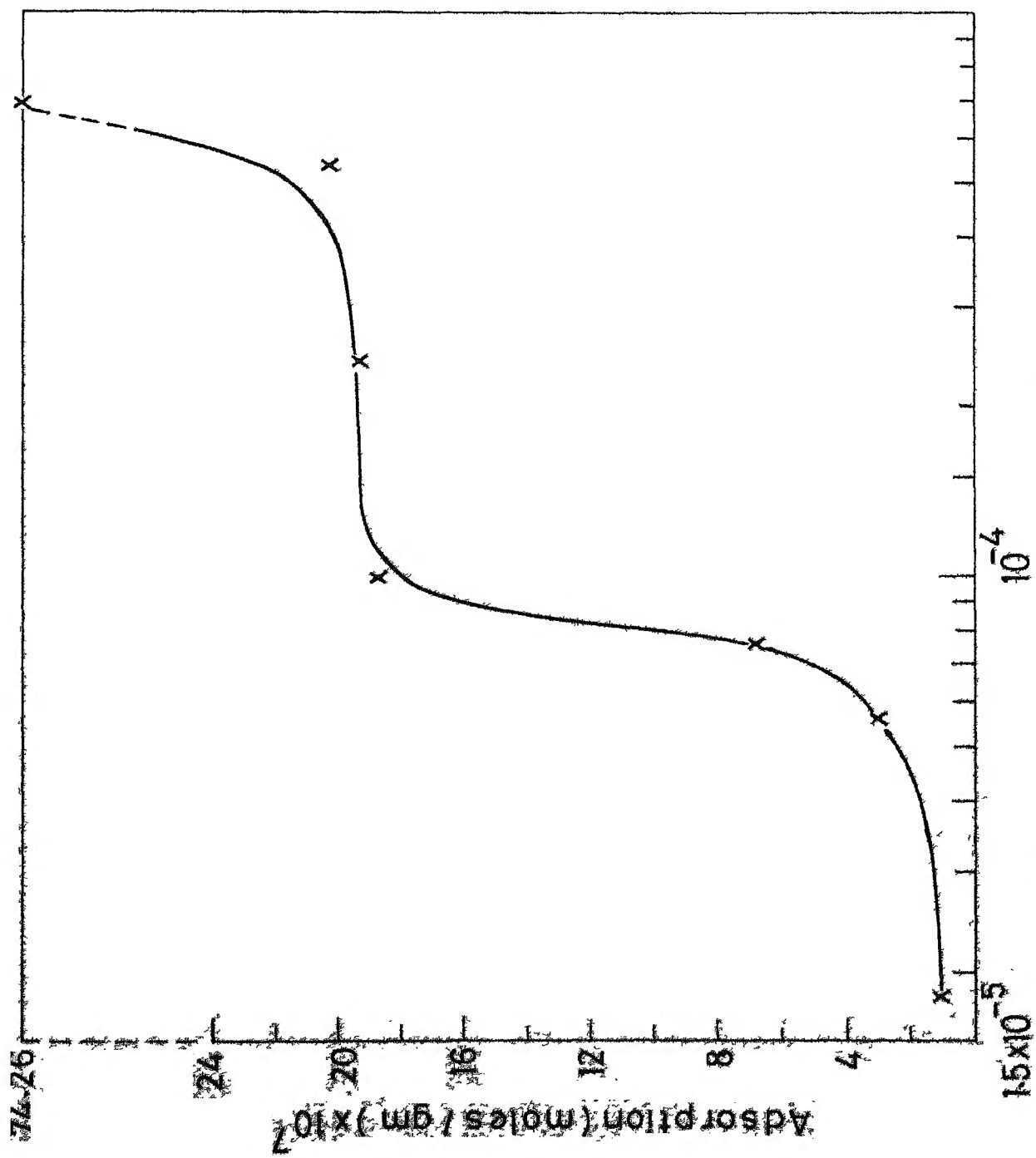
FIG. 1 (b) ADSORPTION ISOTHERM OF P-NITROPHENOL ON Fe_2O_3

Equilibrium concentration of PNP (mole / lit)

Adsorption (moles / gm) $\times 10^7$

For contact angle and three-phase experiments
1 cm. cube corfundum crystal was used This crystal with
(100) planes cut and polished was supplied by Linde Co.,
Chicago, U.S.A.

2.2 Liquids

Double-distilled water, pure dodecane and
distilled kerosene were used for various experiments.

n-dodecane was procured from B.D.H. Chemicals
Ltd., U.K. This was distilled at $215^{\circ}C$. Purity estimated
by gas-liquid chromatography was greater than 99 per cent.
n-dodecane was used for adsorption and three-phase contact
experiments.

Straight-run kerosene obtained from Indian Oil
Corporation Ltd. was allowed to stand for 24 hours over
strong caustic soda solution for removal of fatty acid and
other natural surface-active agents. ~~Subsequently,~~ this
was distilled under reduced pressure (10 mm. of Hg), the
fraction collected between 80° and $120^{\circ}C$ had a natural
b.p. of $200 - 240^{\circ}C$ and was used for liquid-liquid
extraction of fine particles.

2.3 Collector

Sodium myristate was used as collector through-
out the course of the experiments.

The untagged myristic acid was obtained from the Hormel Institute fatty acid project at University of Minnesota, U.S.A. Estimated purity was $>$ 99 per cent as determined by gas-liquid and thin-layer chromatography analysis. The molecular formula of myristic acid is $CH_3(CH_2)_{12}CO_2H$ and the molecular weight 228.36.

Sodium myristate was prepared by the well-known procedure[16,17] of saponification in alcoholic medium, evaporation of alcohol and crystallisation from acetone.

The labelled myristic acid was obtained from the isotope division of Bhabha Atomic Research Centre, Bombay, India. The specific activity of the acid is reported to be 3.27 mC_1/m. mole. The labelled myristic acid was obtained in solid form and was dissolved in benzene.

CHAPTER 3

EXPERIMENTAL PROCEDURES

3.1 Liquid-Liquid Extraction of Fine Particles

150 c.c. of aqueous solution of surfactant was equilibrated for 20 mins. with 1 g. of material to be floated and 75 c.c. of kerosene in the apparatus shown in Fig. 3. Through the piston arrangement about 20 c.c. of kerosene was sucked up from the top layer and then pushed through the 0.7 mm. internal diameter nozzle in aqueous solution in about 1 sec. One experiment consisted of 20 such circulations. Subsequently, the system was allowed to stand by itself for $\frac{1}{2}$ an hour. Then the particles collected at the interface were removed through the side stop-cock, filtered, dried at $120^\circ C$ and weighed The aqueous solution in the bottom of the flask was taken for pH measurements.

3.2 Tracer-Technique for Sodium Myristate Estimation

This technique was employed to estimate labelled sodium myristate, its distribution across water and n-dodecane and its adsorption on mineral surfaces from aqueous and n-dodecane phases.

15 CC Syringe

0.7

0.7

2

15

23

10

9

1
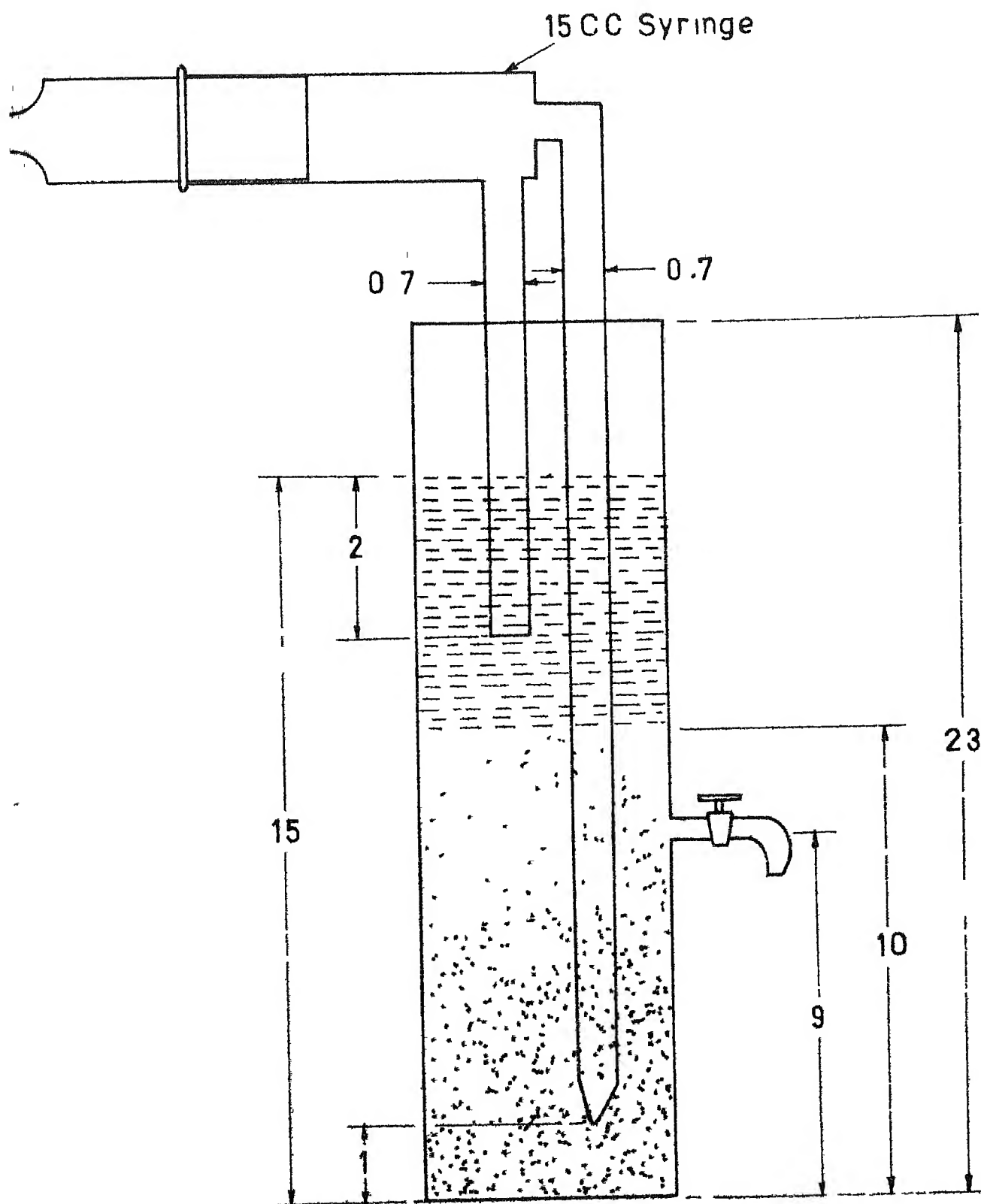
Dimensions are in cm

FIG. 3   LIQUID-LIQUID EXTRACTION APPARATUS

The tracer element carbon-14 used to label myristic acid is a weak β-emitter and has a half-life of 5700 years. The maximum energy of β-range is 0.155 Mev and would penetrate a layer of 0.2 cm. thick myristic acid In the present investigation, the Geiger Muller counting system (GCS-13 of Electronic Corporation of India) has been used. It consists of a high voltage supply, a preset timer and a decade scaler to record the number of counts from the G.M. detector. Fig. 4 shows the characteristic curve for the G.M. detector. Appropriate disc bias and filament voltages were chosen.

3.3 Preparation of Tagged Sodium Myristate Solution

A suitable quantity of tagged myristic acid (7 mg. of labelled myristic acid was dissolved in 10 ml. of benzene and 0.1 ml. of this solution) was taken from the vial to a volumetric flask. Excess of sodium hydroxide solution was added to make the volume around 15 ml. The mixture was kept at 60°C for six hours in a thermostat for frequent shaking. The stopper was frequently opened to allow the benzene vapour to escape. At the end of this period of saponification, the resulting solution was added to a solution of untagged sodium myristate. The ratio of tagged to untagged was 5.170 or 1.34 as maintained through the course of various experiments.
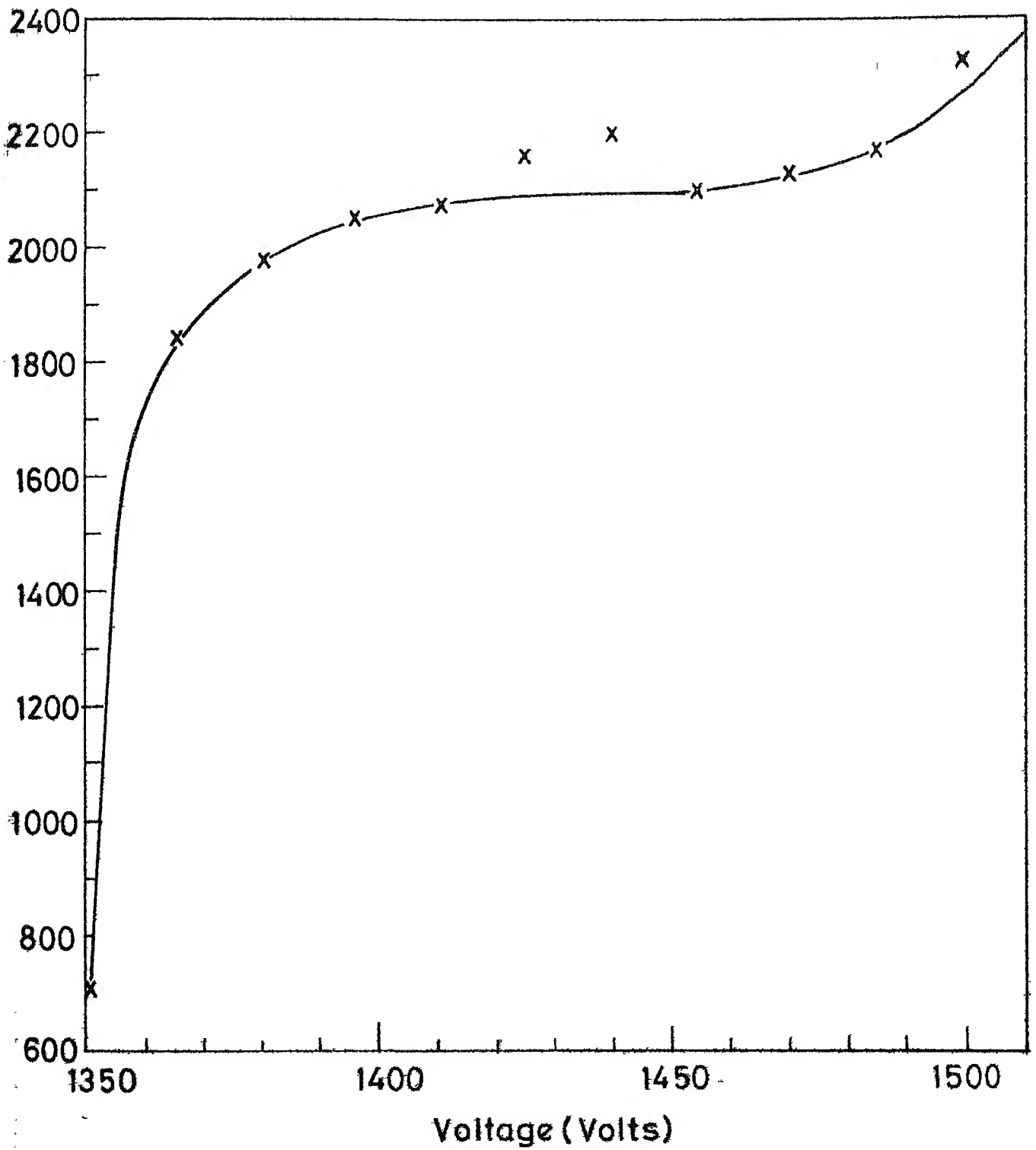
FIG. 4   CHARACTERISTIC CURVE FOR GM DETECTOR

3.4 Standard Curves

2 ml. of solutions of different concentrations were evaporated to dryness on stainless steel pans These were placed directly under the G.M. counter and the total number of counts were noted Necessary background corrections were made. Standard calibration curves were obtained for different pH values. Using these calibration curves (vide Figs. 5-7) solute was estimated in solutions of unknown concentrations.

3.5 Distribution of Sodium Myristate Between n-Dodecane and Water

30 ml. of aqueous solutions of sodium myristate were equilibrated at different pH with 10 ml. of n-dodecane at $30 \pm 1^{\circ}C$ for 6 hrs. The aqueous solution contained tagged myristic acid in proportions mentioned earlier. After equilibration, concentrations in different phases were estimated after evaporation of 2 ml. of solution and using the G.M. counter and the calibration curves.

3.6 Adsorption Measurements

10 ml. of aqueous solution of sodium myristate previously equilibrated with dodecane were used. One gram of powder was shaken vigorously with the solution for
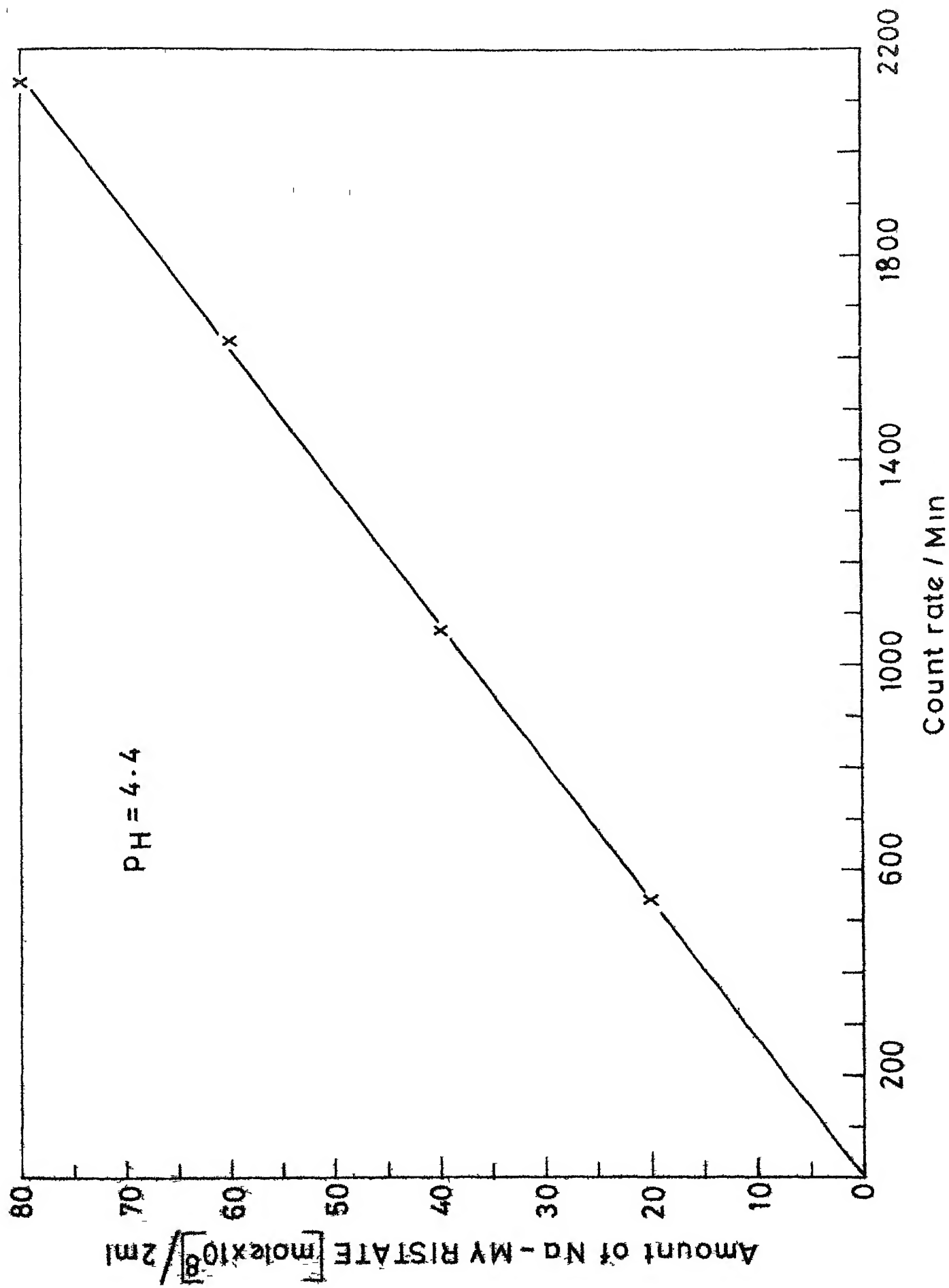
FIG. 5 STANDARD CURVE FOR ESTIMATION OF Na - MYRISTATE BY C₁₄ TRACER

Amount of Na-MYRISTATE [mole x 10⁸/2 ml]
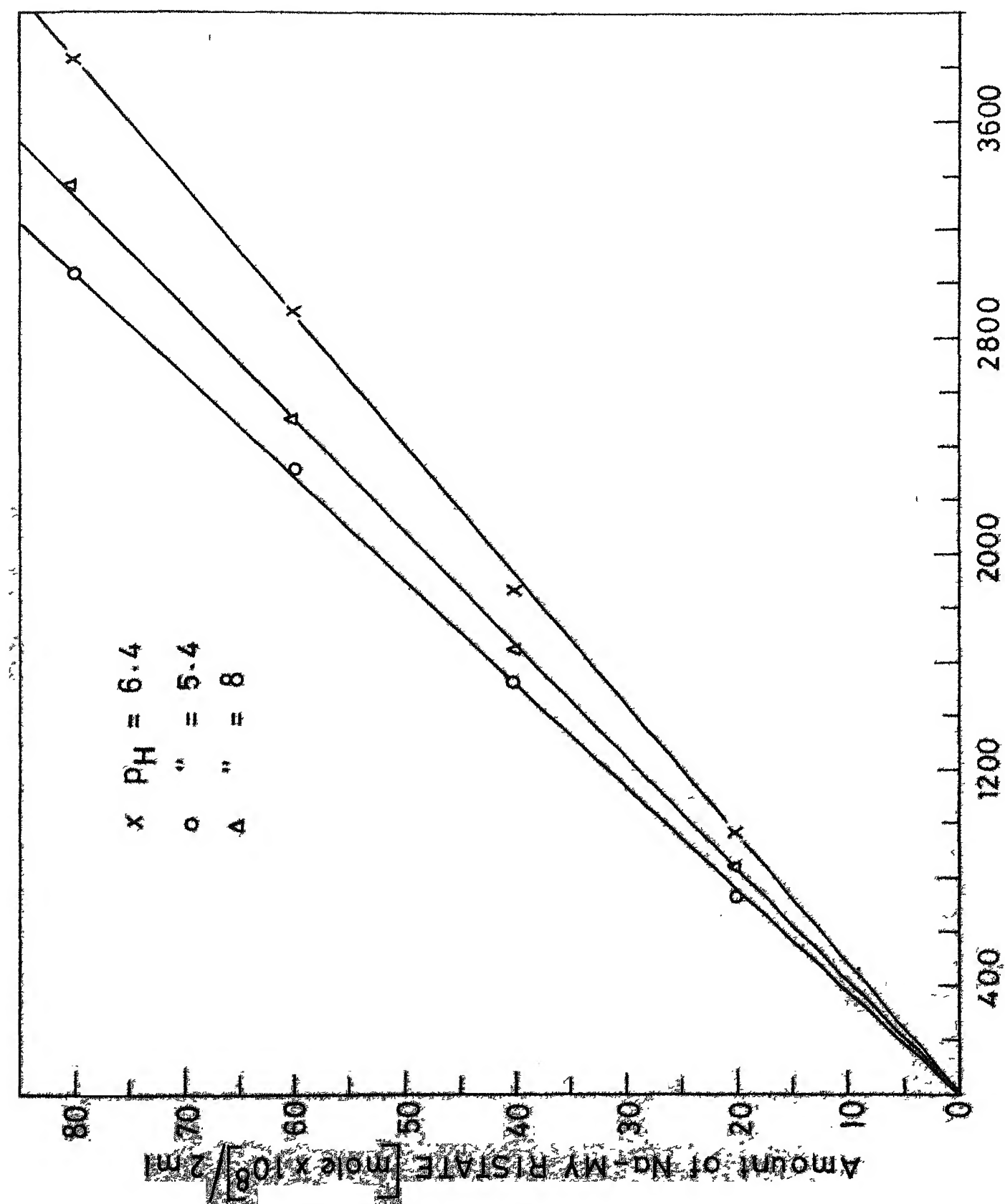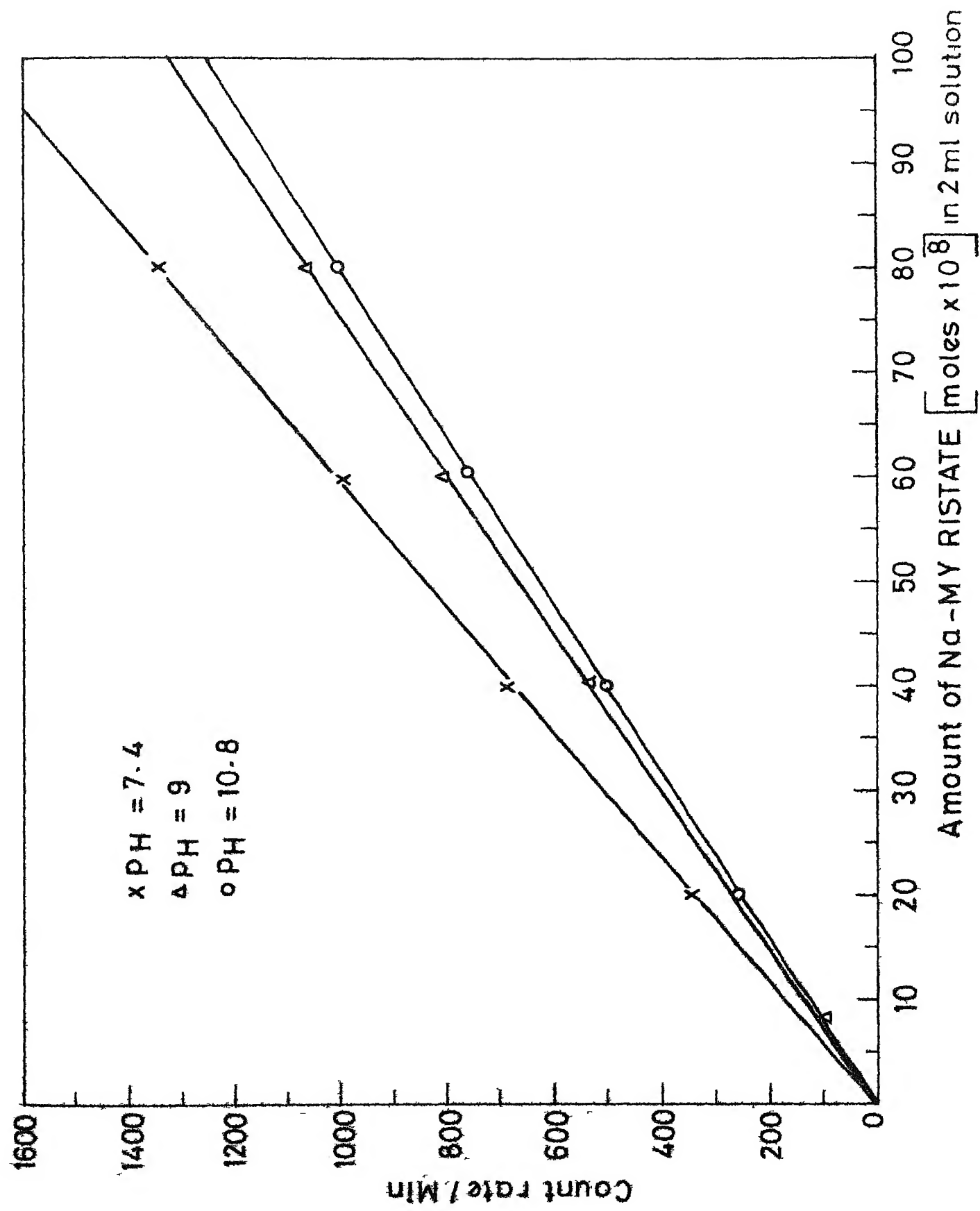
$\frac{1}{2}$ an hour and kept at 30 ± 1°C in a ~~thermostat~~ for six *Thermostatically controlled water bath*
hours. The supernatant liquid was taken out with a
pipette and centrifuged at 1500 r.p.m. Two ml. of the
clear solution were transferred to the stainless steel pan
for estimation of equilibrium concentration after adsorp-
tion. The amount adsorbed could be calculated from the
difference in concentrations.

Similarly, 5 ml. of the equilibrated dodecane
phase were used together with 0.5 g. of oxide powder for
adsorption experiments.

3.7 Three-Phase Interline Adsorption Experiments

Thoroughly cleaned corundum crystal was placed
in a cuvette which contained 25 ml. of tagged sodium
myristate solution whose concentration and pH were known.
One drop of equilibrated dodecane ($\sim \frac{1}{2}$ c.c.) was made to
attach on the solid surface by a bubble holder. After
allowing sufficient time for stable contact ($\frac{1}{2}$ an hour),
the crystal was then taken out of the cuvette (when the
bubble also got detached). In certain experiments, the
entire surface was rinsed with small quantity of water
($\sim$ 1 c.c.) and in some other experiments, the crystal was
not rinsed but merely tilted for free draining of super-
ficial liquids. In all cases, the crystals were dried

and then mounted on the base of a travelling microscope
which had a least count of 0.01 mm.

G.M. counter tube, which had a lead disc, with
a fine hole of 0.004 inch was attached at the bottom, and
the whole assembly was mounted on a perspex stand. The
entire surface of the crystal was scanned by moving the
crystal under the G.M. tube along a diameter. The
absolute count rates were obtained at different distances
from one end. These were taken as measures of local
adsorption densities.

3.8 Contact Angle Experiments

For the measurement of contact angles, captive
bubble technique was used. Sodium myristate solution
which had been equilibrated with dodecane was taken in a
cuvette and the single crystal of corumdum was submerged
in it. A drop of equilibrated dodecane was placed on the
crystal by a bubble holder. The image of the bubble was
projected on a flat paper surface, and the contact angles
were measured by drawing tangents and measuring the angle
in the aqueous phase between the tangent and the projected
interline.

CHAPTER 4

EXPERIMENTAL AND SOME COMPUTED RESULTS

4.1 Extraction of Particles at the Water-Kerosene Interface

Liquid-liquid extraction experiments were performed as described under Section 3.1. Solid particles used were (a) fine alumina 0.5 - 9 micron size (vide Fig. 1) (b) same fine alumina particles washed with acetone and dilute HCl to free the surface from any possible impurity (c) coarse alumina 5 - 60 micron size (vide Fig. 2) (d) rutile and (e) Fe_2O_3 particles size distribution of which are given in Tables 1 and 3 and Fig. 1.

(a) Recovery without any collector

Tables 4-7 and Figs. 8-9 contain the data on recovery of Al_2O_3 (washed, unwashed fine and coarse), TiO_2 and Fe_2O_3 particles in the water-kerosene interface without any collector at different pH values of the aqueous system. Reproducibility of recovery was ± 2 per cent. For Al_2O_3, it was observed that emulsion gets stabler at higher pH particularly above 7.0. Around 7.5 pH fine particles form some clusters at the interface. With coarse Al_2O_3 particles, emulsion stability is less and maximum around

X Fine Al_2O_3
O Fine Al_2O_3(washed)
△ Coaase Al_2O_3

Emulsion not stable

Very less emulsion

Emulsi very stable

Stable emulsion

Less emulsion

Moderate emulsion

pH
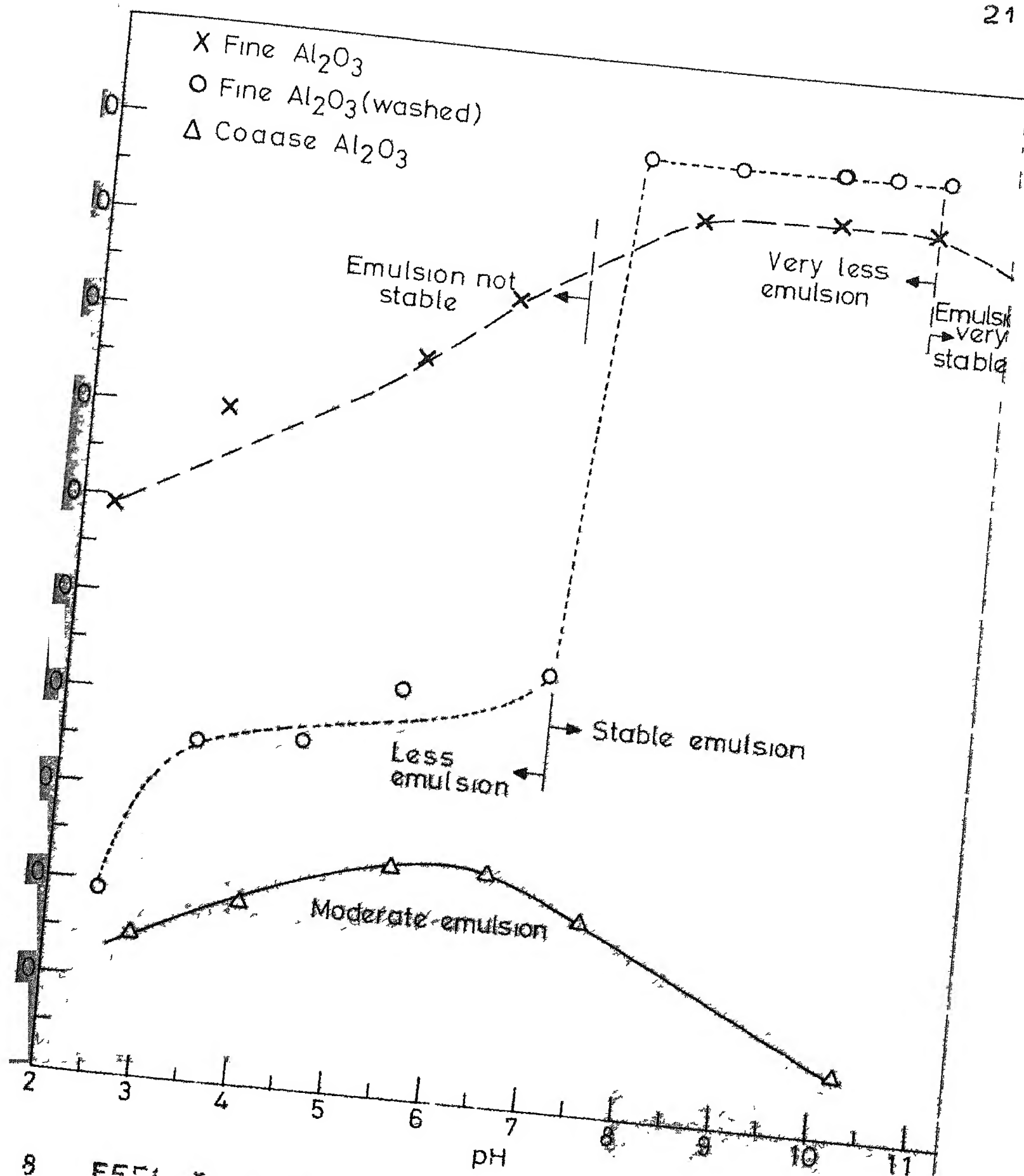
8 EFFECT OF PH ON THE RECOVERY OF Al_2O_3 WITHOUT COLLECTOR
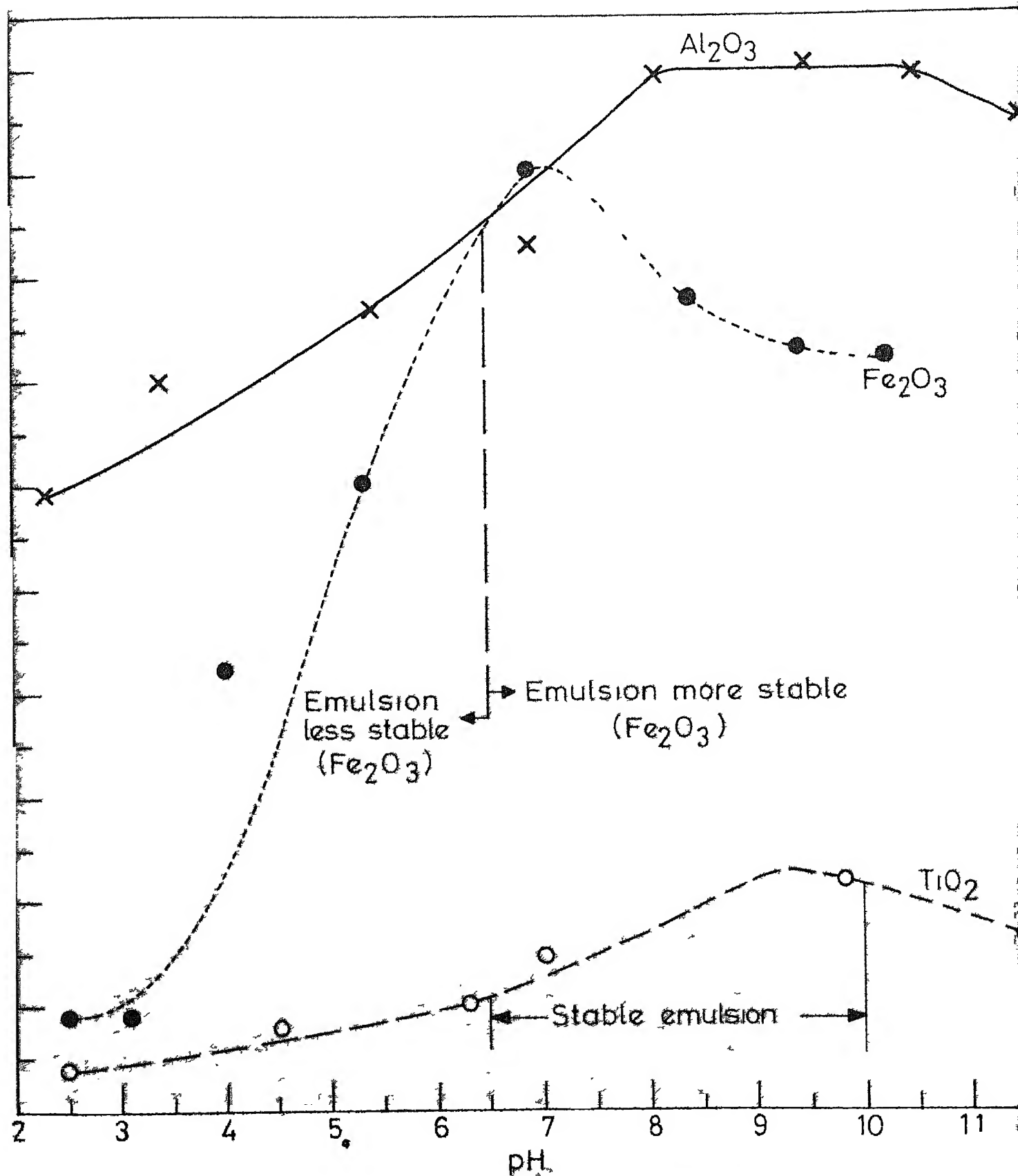
FIG 9 EFFECT OF pH ON THE RECOVERY Al₂O₃, Fe₂O₃ & TiO₂ WITHOUT COLLECTOR

pH 6.0. Recovery is also less. With Fe_2O_3, recovery is maximum at a pH of around 7.0. Emulsion gets stabler above 6.5 pH. For rutile, recovery is much less compared to Al_2O_3 and Fe_2O_3. Emulsion stability is maximum in the pH range 6.5 - 10.0.

(b) Recovery with increase in collector concentration

Tables 8-11 and Figs. 10-11 show the effect of increasing concentration of sodium myristate in the aqueous phase on increasing recovery of the particles. For Al_2O_3 and TiO_2 emulsion stability was found to increase with increasing collector concentration. Around 10^{-4} m/l. concentration, formation of clusters was observed. Copious emulsion at high pH and collector concentration gave poorer reproducibility of the p.c. recovery ($\pm$ 10%). For Fe_2O_3 at higher collector concentration ($>$ 2 x 10^{-4} m/l.), clusters get bigger at the interface, trap a large amount of kerosene. This kerosene-Fe_2O_3 sludge sinks at the bottom of the aqueous phase and explains the decrease in recovery of Fe_2O_3 with increasing collector concentration.

Dilution tests clearly show that the emulsions are O/W type and the sludge is essentially an oily phase.

(c) Recovery as a function of pH in presence of collector

Tables 12-16 and Figs. 12-13 contain the data related to recovery of oxide particles in the liquid-liquid
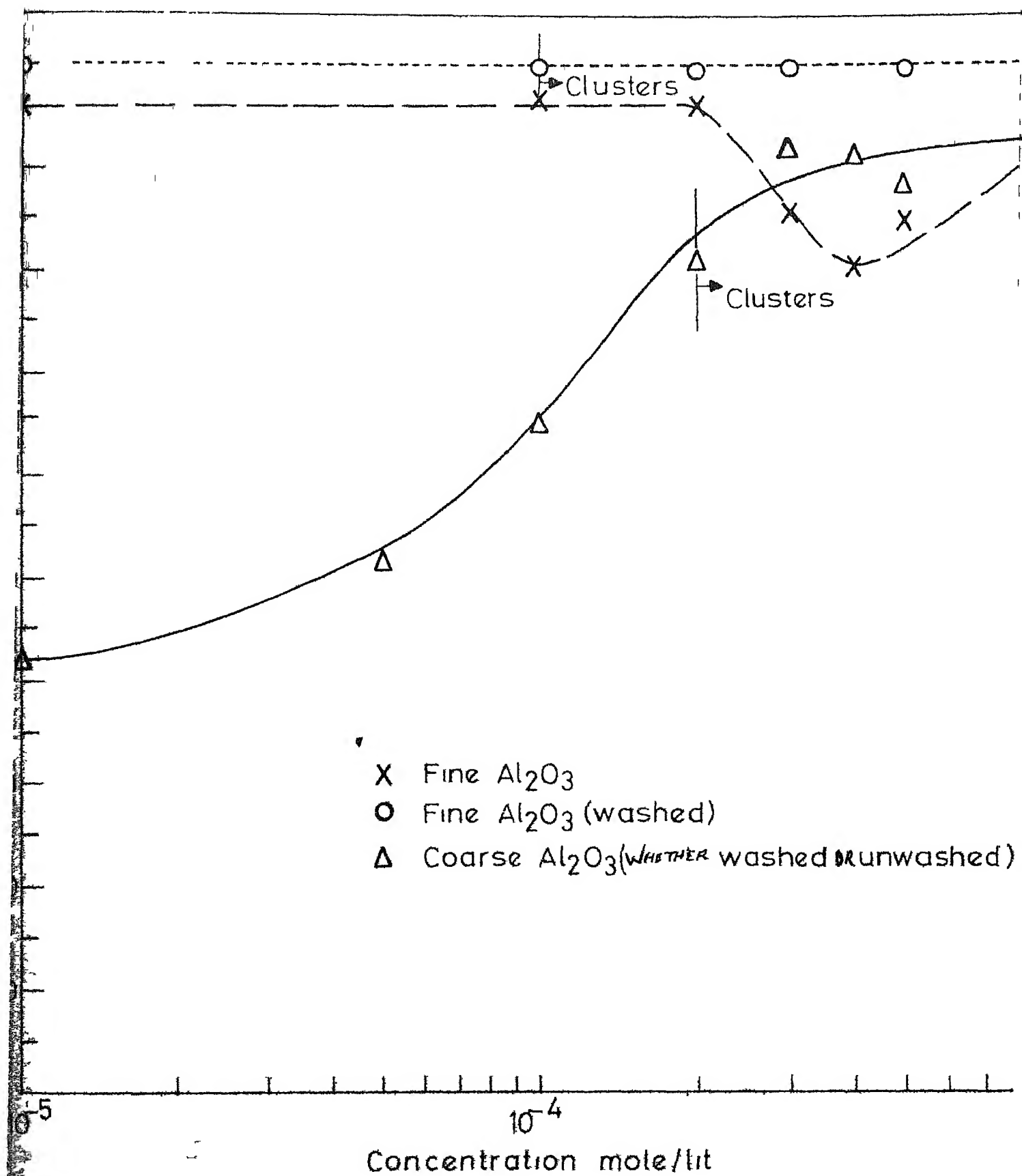
Clusters

Clusters

X   Fine Al_2O_3
O   Fine Al_2O_3 (washed)
△   Coarse Al_2O_3(WHETHER washed OR unwashed)

0^{-5}

10^{-4}

Concentration mole/lit

FIG.10   EFFECT OF COLLECTOR CONCENTRATION ON THE RECOV
OF Al_2O_3

X Al_2O_3

O Fe_2O_3

△ TiO_2

Formation of sludge
with organic phase
(Fe_2O_3)

For TiO_2 emulsion stabler
at high con

2x10^{-5} 10^{-4} 2   3   4   5   6 7 8

Collector concentration mole/l
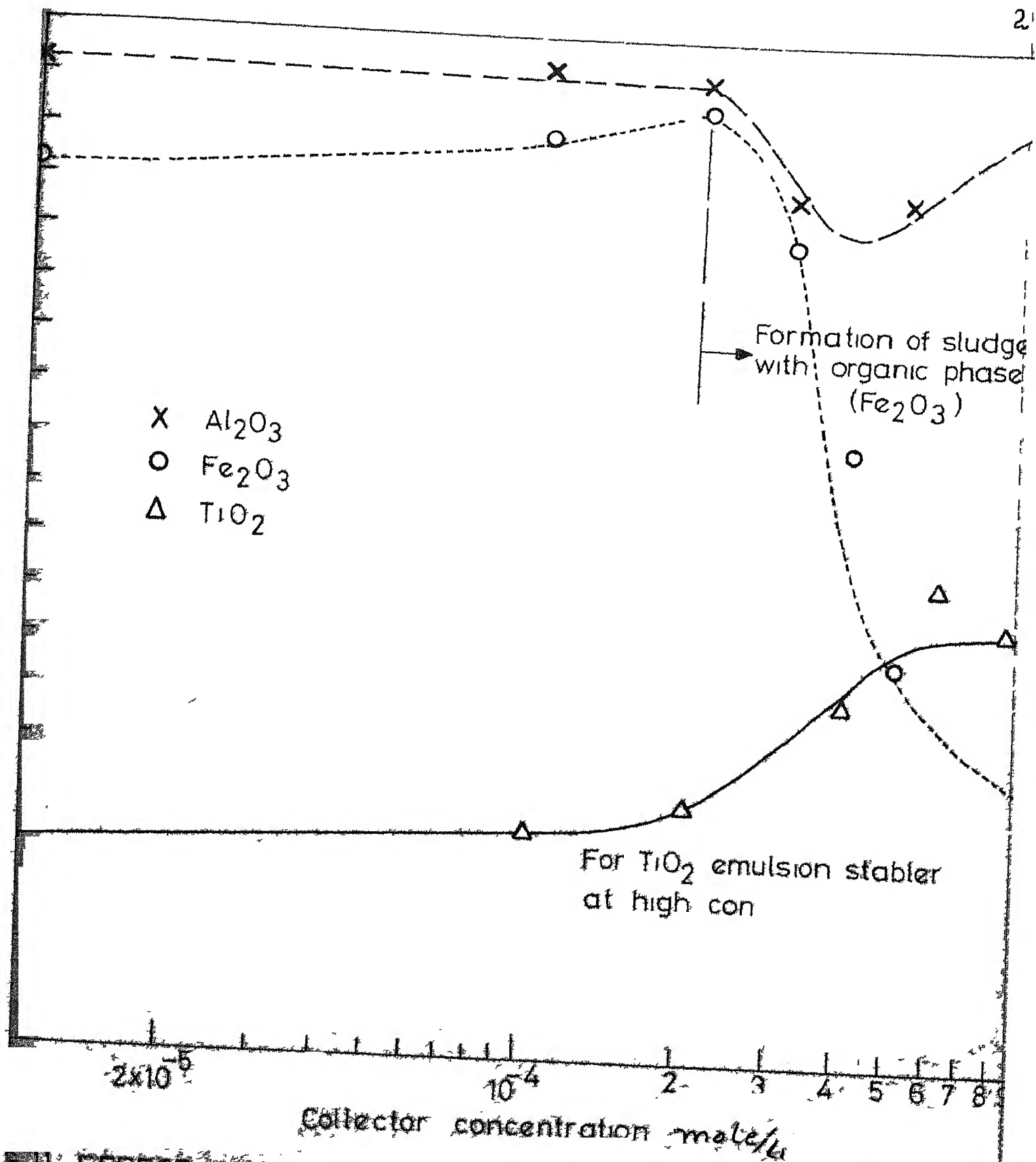
p 11 EFFECT OF COLLECTOR CONCENTRATION ON THE RECOVERY
Al_2O_3, Fe_2O_3 & TiO_2 IN PURE SYSTEMS

Collector concentration = 2×10^{-4} mole/lit

Clusters ← → Stable emulsion

Emulsion not stable ←

Stable emulsion

Clusters ←

X Fine Al_2O_3
O Fine Al_2O_3 (washed)
Δ Coarse Al_2O_3 (WHETHER washed or unwashed)

pH
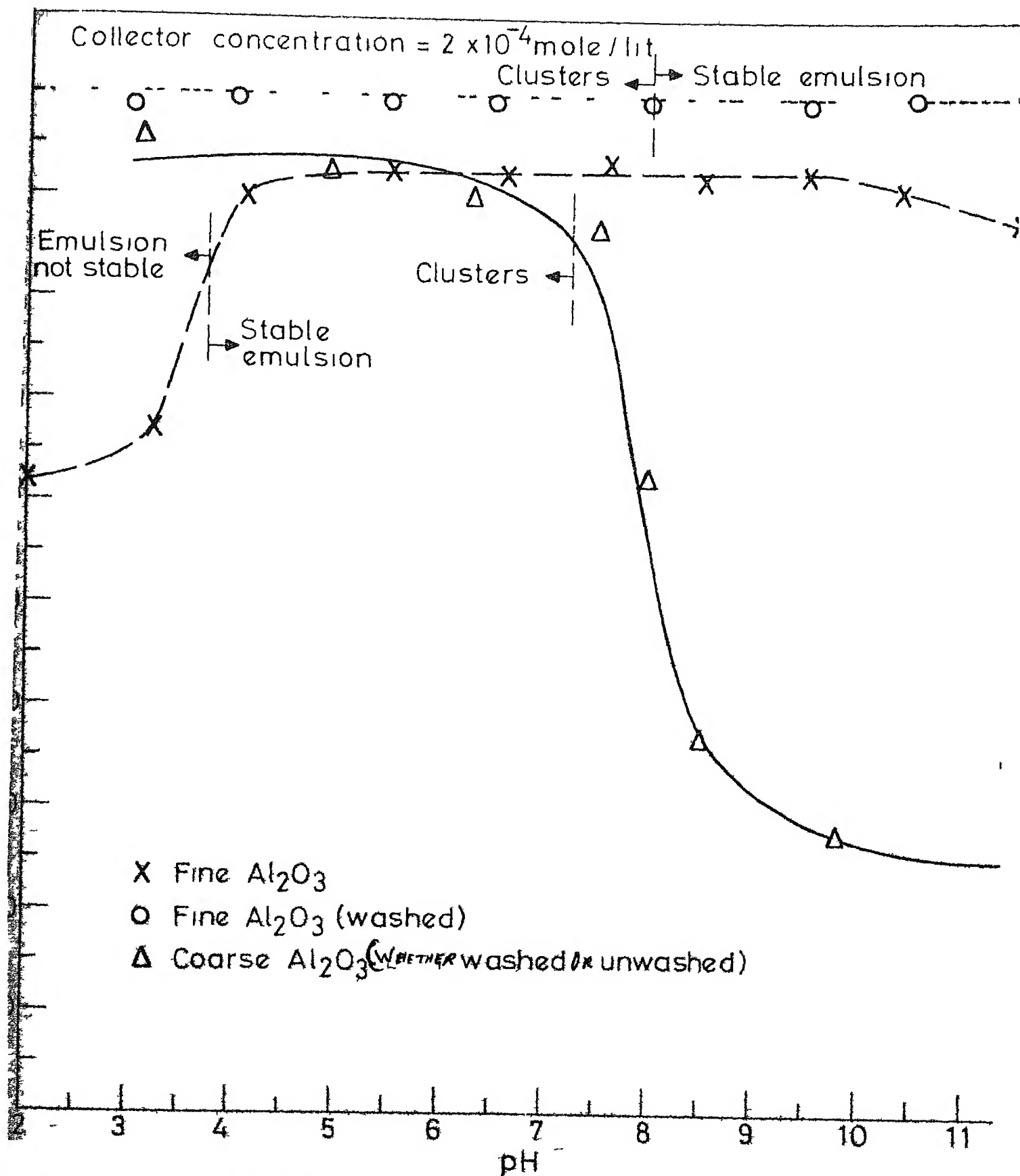
FIG. 12 — EFFECT OF pH ON THE RECOVERY OF Al_2O_3 IN PRESE OF COLLECTOR

Collector concentration = 2×10^{-4} mole/l

Cluster
no emulsion
(Fe_2O_3)

Emulsion
(Fe_2O_3

Less
emulsion

More stable emulsion

Less
emulsion

O Fe_2O_3
Δ Al_2O_3
X TiO_2

pH
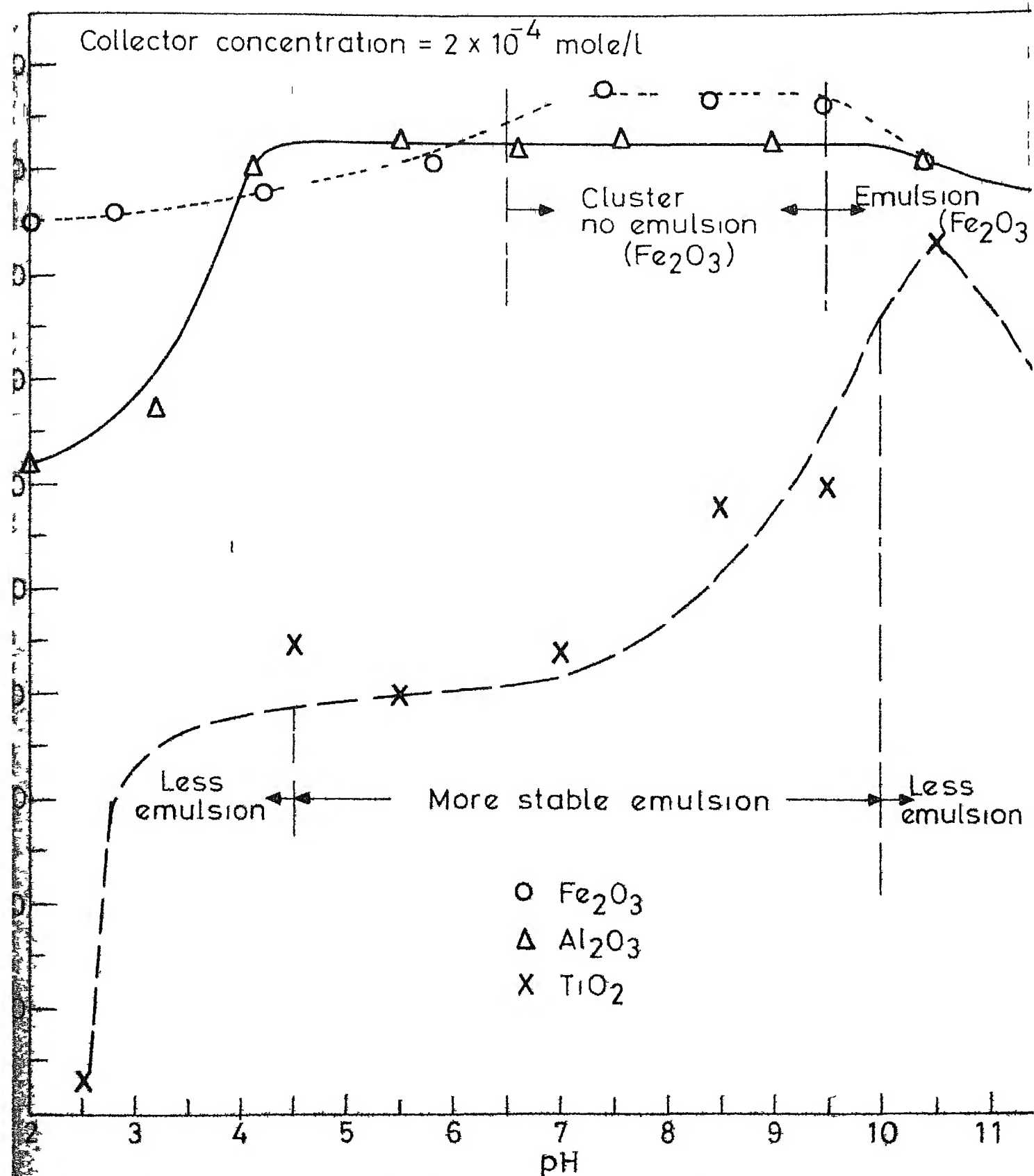
13   EFFECT OF pH ON THE RECOVERY OF Al_2O_3, Fe_2O_3 &
    TiO_2 IN PRESENCE OF COLLECTOR

interface in presence of collector as a function of pH.

With Al_2O_3, there is substantial cluster formation upto pH 8.0 above which there is less cluster, and emulsion gets stabler. With Fe_2O_3 there are clusters and little emulsion in the pH range 6.5 - 9.5 above which emulsion becomes stabler. With TiO_2, maximum recovery is at pH 9.0 - 9.5 and pH 10.5 when the collector concentrations are 4 x 10^{-5} (Fig. ~~13b~~ 26) and 2 x 10^{-4} m/l. respectively. With more collector concentration, the pH range for emulsion stability becomes wider.

(d) Attempts for separation of Al2O3/Fe2O3 through the use of the above technique

Figs. 9, 11 and 13 show that Al_2O_3/Fe_2O_3 separation may be marginally possible under certain conditions e.g. (1) no collector and extreme pH such as 3.0 or 10.0 (ii) high collector concentration such as 10^{-3} m/l. at neutral pH which would however involve lot of consumption of collector as well as kerosene (iii) use of collector and low pH. It is also clear however that in the neutral range of pH and moderate sodium myristate concentration behaviour of Al_2O_3 and Fe_2O_3 are similar.

Some experiments were performed with 50:50 (by weight) mixture of Al_2O_3 and Fe_2O_3. Results shown in Table 17 confirm the difficulty in separation of Al_2O_3

from Fe_2O_3 using the present system. If the present technique has to be used for beneficiating high alumina iron-ore, then some other specific collector should be investigated.

4.2 Distribution of Surfactant (Sodium Myristate/Myristic Acid) Across Water and n-dodecane

Following the procedure outlined in Section 3.5, surfactant distributions across the two phases were determined at different pH values

Assuming myristic acid to be compatible in both the phases and myristate ion in the aqueous phase only, we may write

$$K_D = \frac{[RCOOH]_O}{[RCOO^-]_W + [RCOOH]_W} \qquad (1)$$

and

$$D = \frac{[RCOOH]_O}{[RCOOH]_W} \qquad (2)$$

where subscripts 'O' and 'W' refer to the organic and aqueous phases. If the model is valid, then D (but not K_D) should be constant at a particular temperature and independent of pH.

We may further write:

$$K_D = \frac{D}{1 + \dfrac{[RCOO^-]_W}{[RCOOH]_W}} = \frac{D}{1 + \dfrac{1}{K_a[H^+]}} \qquad (3)$$

where $\qquad K_a = \dfrac{[RCOOH]_W}{[RCOO^-]_W[H^+]_W} \qquad (4)$

for the reaction $\qquad RCOOH \longrightarrow RCOO^- + H^+$

$$K_a = \frac{K_h}{K_w} \qquad \text{where} \qquad K_h = \frac{[RCOOH]_W[OH^-]_W}{[RCOO^-]_W}$$

K_h is $(0.63 - 1.56) \times 10^{-9}$ at $25^{\circ}C$ according to Powney and co-workers[18,19].

When pH is low, say 4 then K_a being $\sim 10^5$ $\dfrac{1}{K_a H^+}$ is < 1 and hence $K_D \sim D$. On the other hand for very high pH > 5, (say 7-8) $1/K_a H^+$ is $\gg 1$ and hence $K_D = K_a H^+ \cdot D$.

Tabulated data (Table 18) and Fig. 14 show variation of K_D as a function of pH and also the values of D at different pH. Wide variation of D with pH indicates that the above model is not fully valid.

4.3 Adsorption of Sodium Myristate/Myristic Acid from Aqueous and Dodecane Phases

Adsorption measurements were made following the procedure given in Section 3.6. The various results
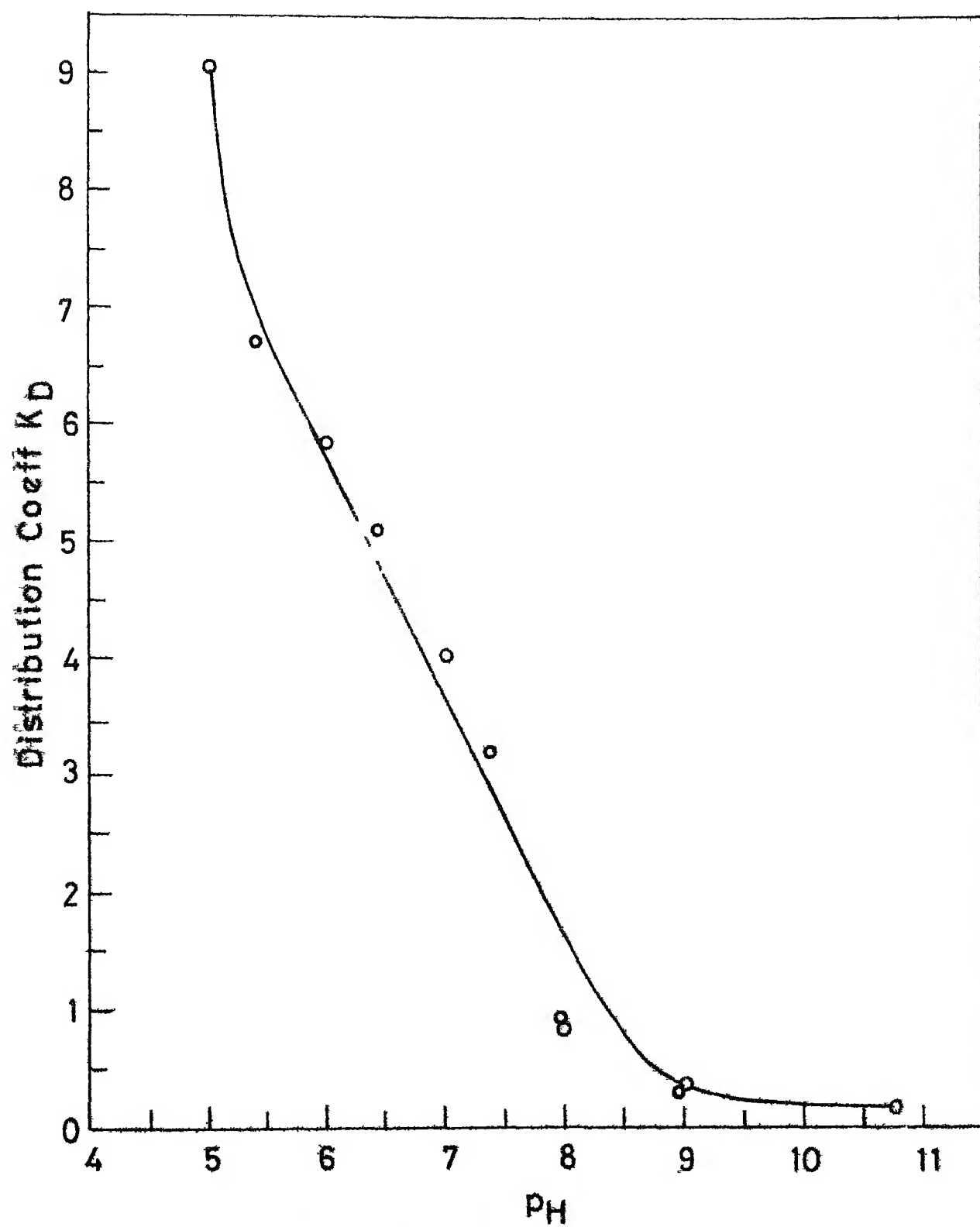
FIG 14 EFFECT OF PH ON DISTRIBUTION COEFF K_D

are given in Tables 19-21 and Figures 15-19   Similar

adsorption daca on rutile compiled by Bhargava[16] are given

in Fig   20 [footnote-θ]

4 4 Adsorption Across Three-Phase Interline

Figs   21-22 contain the information on the

radioactive counts per minute (direct measures of adsorption

density) across the three-phase interline 1 e   on the

solid-water interface, the interline — where the three phases

meets and the solid-dodecane drop interface   The

techniques has been described in Section 3 7   Relative

adsorption density values on the corumdum surface (Γ_W from

the aqueous phase, Γ_O from the organic phase and Γ_1 on the

interline) are tabulated in Table 22 and compared with

equilibrium adsorption data — **given** in Fig   19 and

Tables 19-21

4 5 Contact Angle Measurements

Adopting the technique outlined in Section 3 8,

contact angle measurements were made on corundum crystal-

water-dodecane-sodium myristate system at different pH

and collector concentrations   The data are given in

Fig   23 and Table 23 [footnote-θθ]

[footnote-θ] **If we consider the reproducibility in the case of adsorption
experiments, it is of the order of ±10 percent**

[footnote-θθ] **The reproducibility in the case of contact angle is very
good it is of the order of ±5 percent.**

FIG 15   ADSORPTION ISOTHERM OF Na-My ON Al$_2$O$_3$ FROM WATER PHASE

Concentration of Na–My [mole/lit]

Moles adsorbed /gm of $Al_2O_3 \times 10^8$

x $P_H = 5.4$

o $P_H = 6.4$
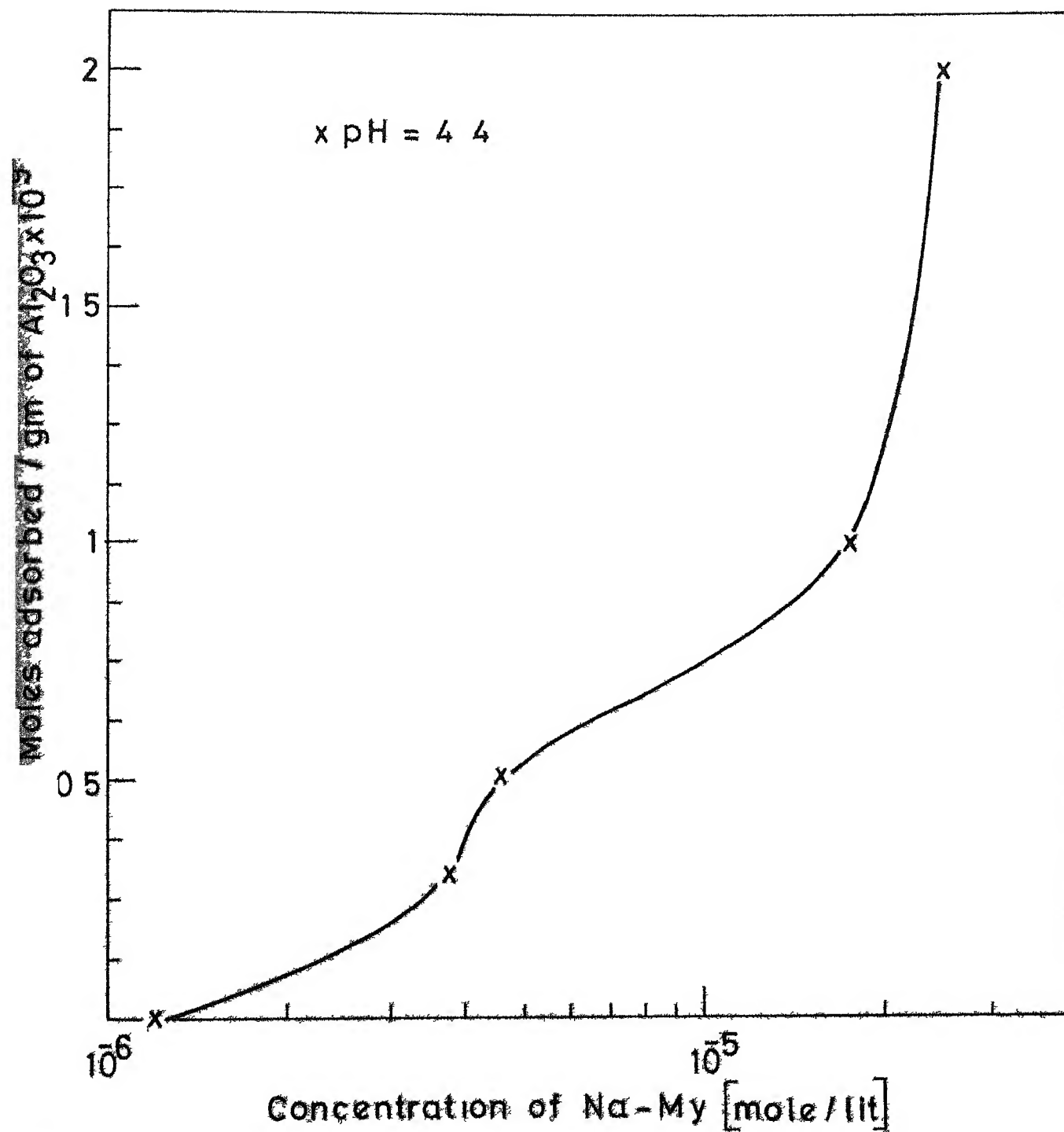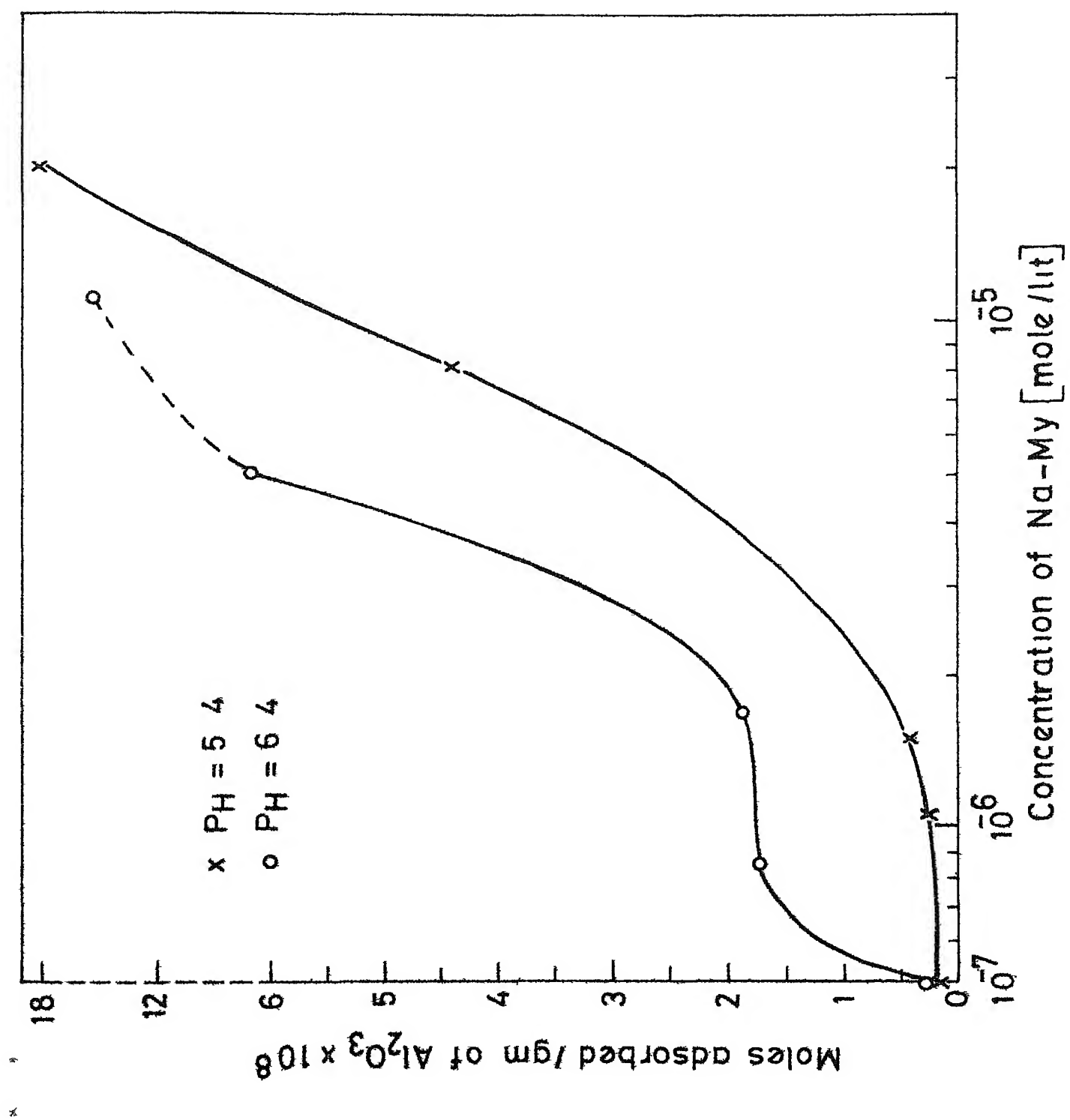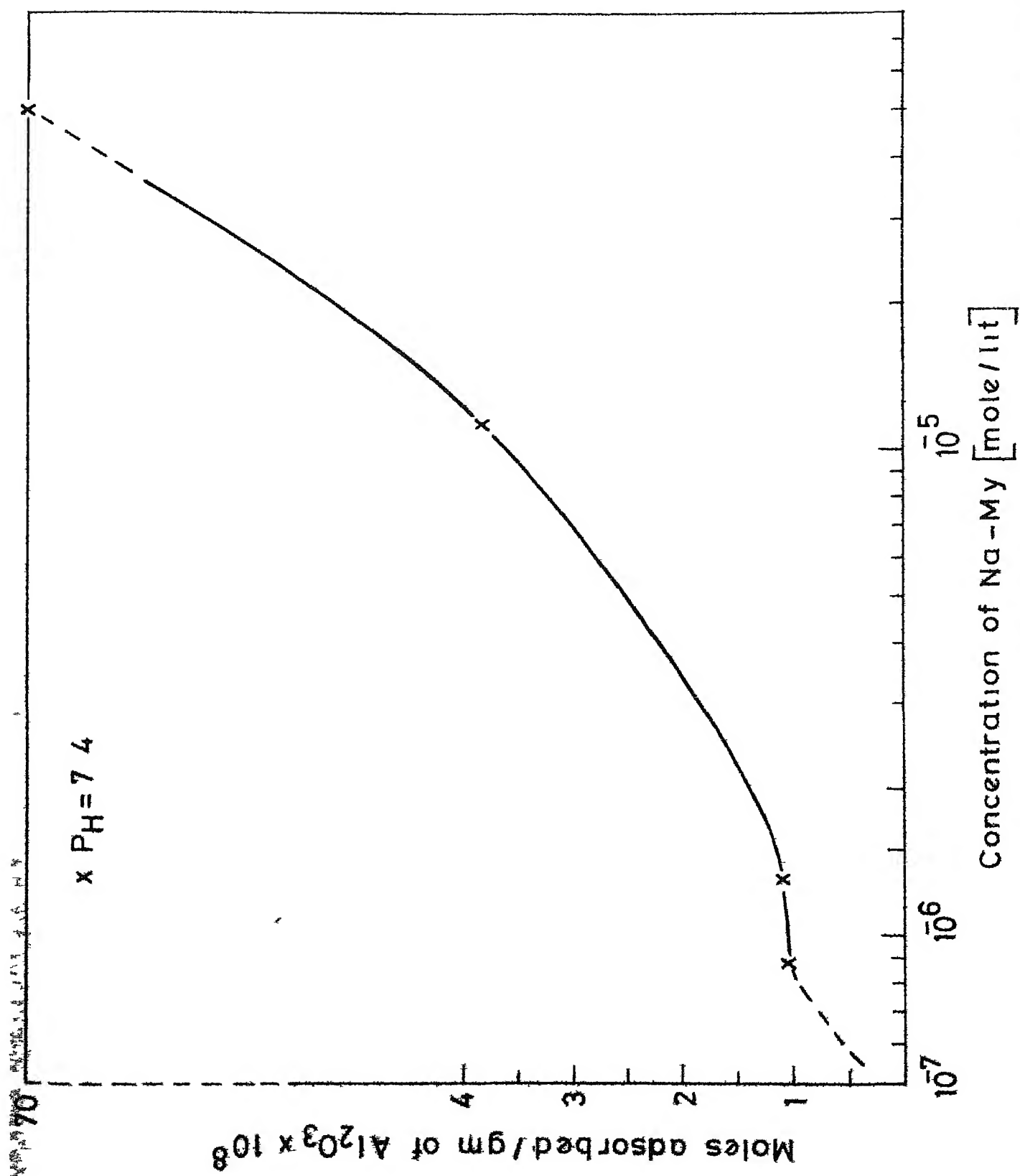
FIG 17   ADSORPTION ISOTHERM OF Na-My ON Al_2O_3 FROM WATER PHASE

FIG 18 ADSORPTION ISOTHERM OF Na–My ON Al$_2$O$_3$ FROM WATER PHASE

10^{-9}

10^{-10}

10^{-11}

10^{-12}

10^{-13}

Aqueous phase equilibrated wit
n-dodecane
4 4 □ pH   8 0 ◇ pH
5 4 △ ,   9 0 ⋈ '
6 4 ▽ "   10 8 ○
7 4 ⋈ ↓

n-Dodecane equilibrated with
Aqueous phase
Similar symbols except filled

Equilibrium concentration of surfactant in mole/lit

10^{-7} 10^{-6} 10^{-5} 10^{-4}
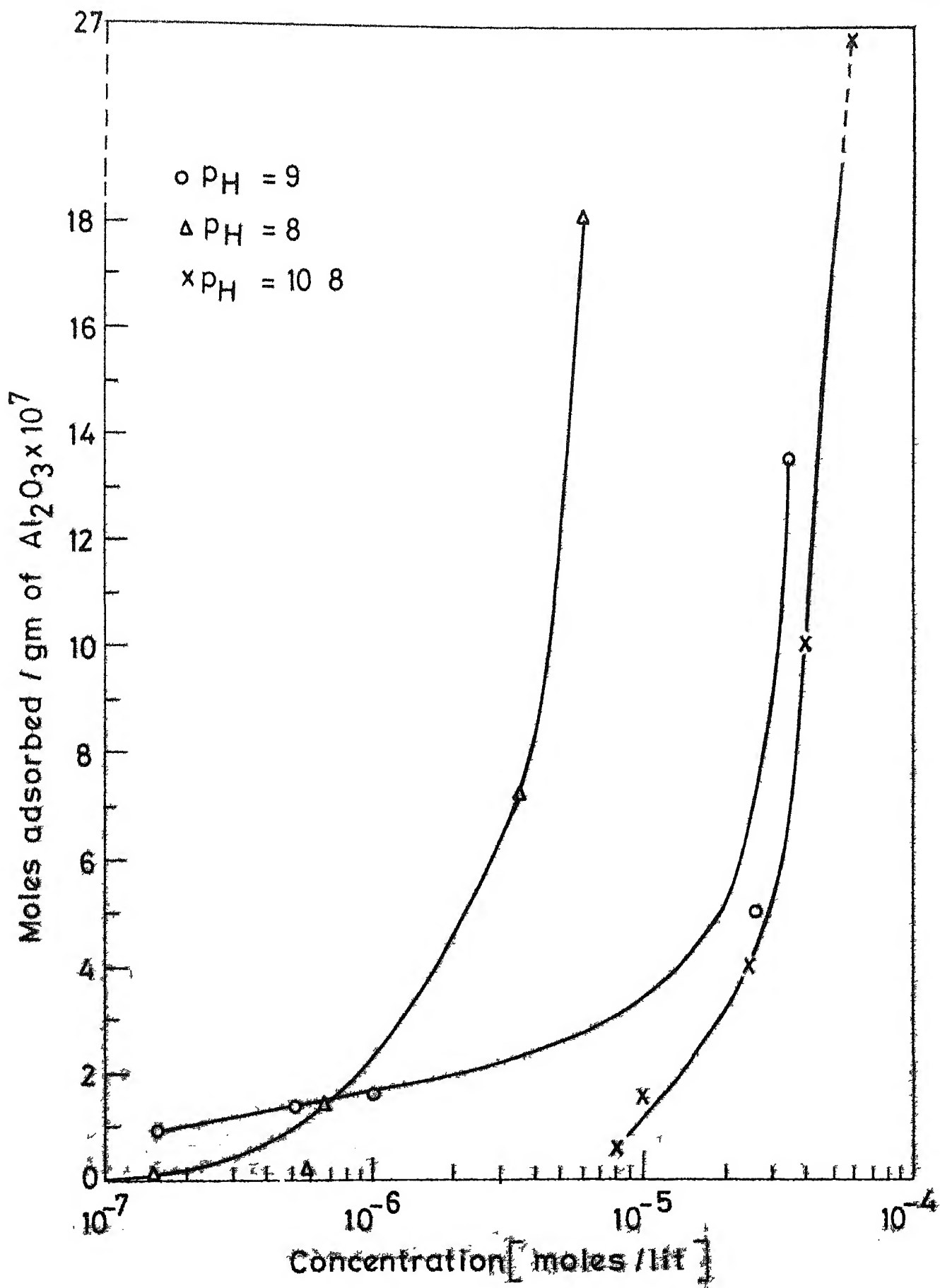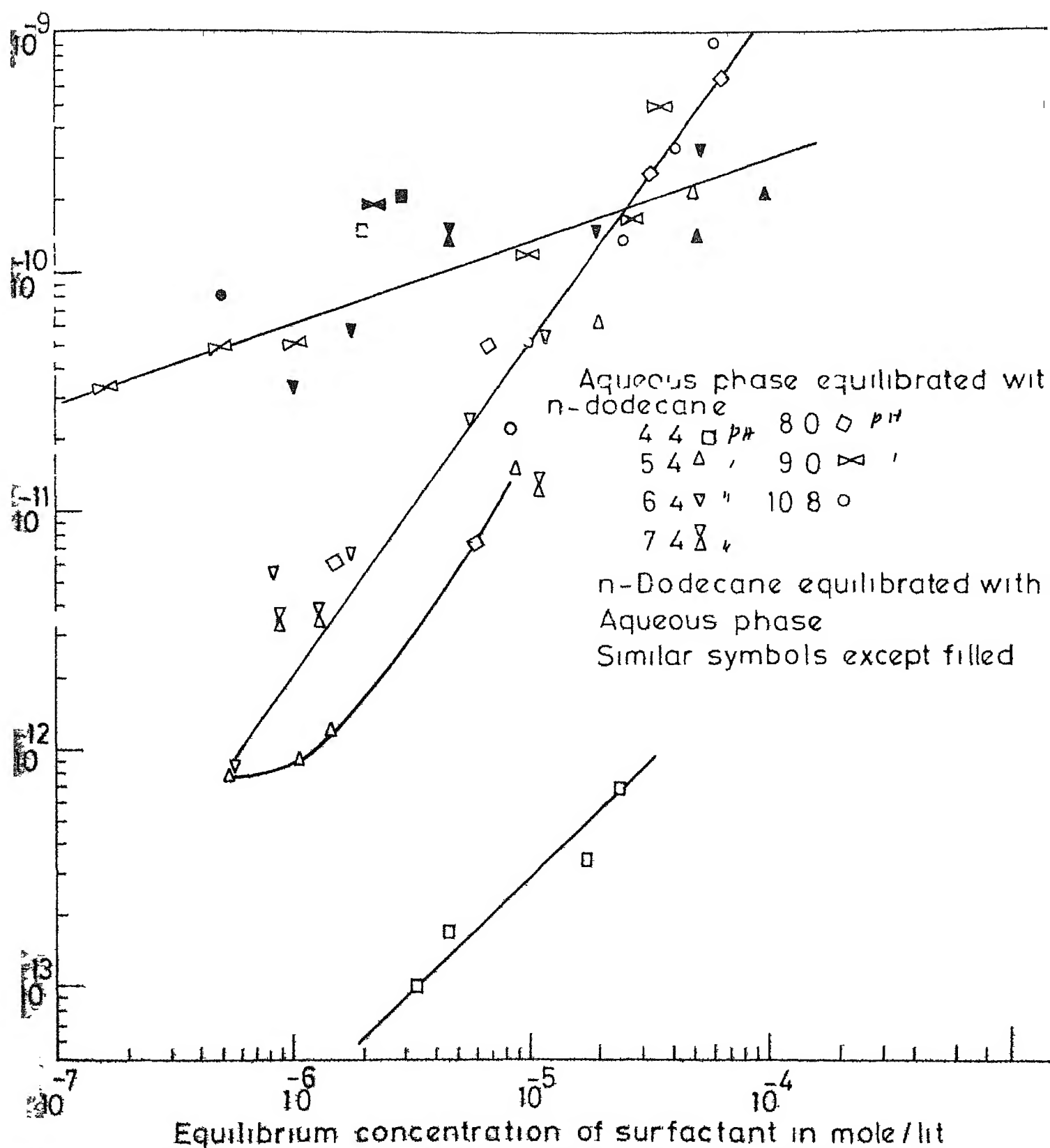
19 ADSORPTION ISOTHERM OF SODIUM MYRISTATE/MYRISTIC ACID
ON ALUMINA FROM ORGANIC & AQUEOUS PHASES

Adsorption of myristic acid / sodium salt mole/cm^2

-10

-11

-12

-13

10^{-10}

10^{-11}

10^{-12}

10^{-13}

□ 5 0 PH
△ 6 0
▽ 7 0 '
◊ 8 0 "
○ 9 0 "

Aqueous phase equilibrated with
n-Dodecane (Negligible adsorption
at pH 5 0 & 9 0)

n-Dodecane equilibrated with
Aqueous phase similar symbols
except filled

10^{-7} 10^{-6} 10^{-5} 10^{-4}

Equilibrium concentration of surfactant mole /l
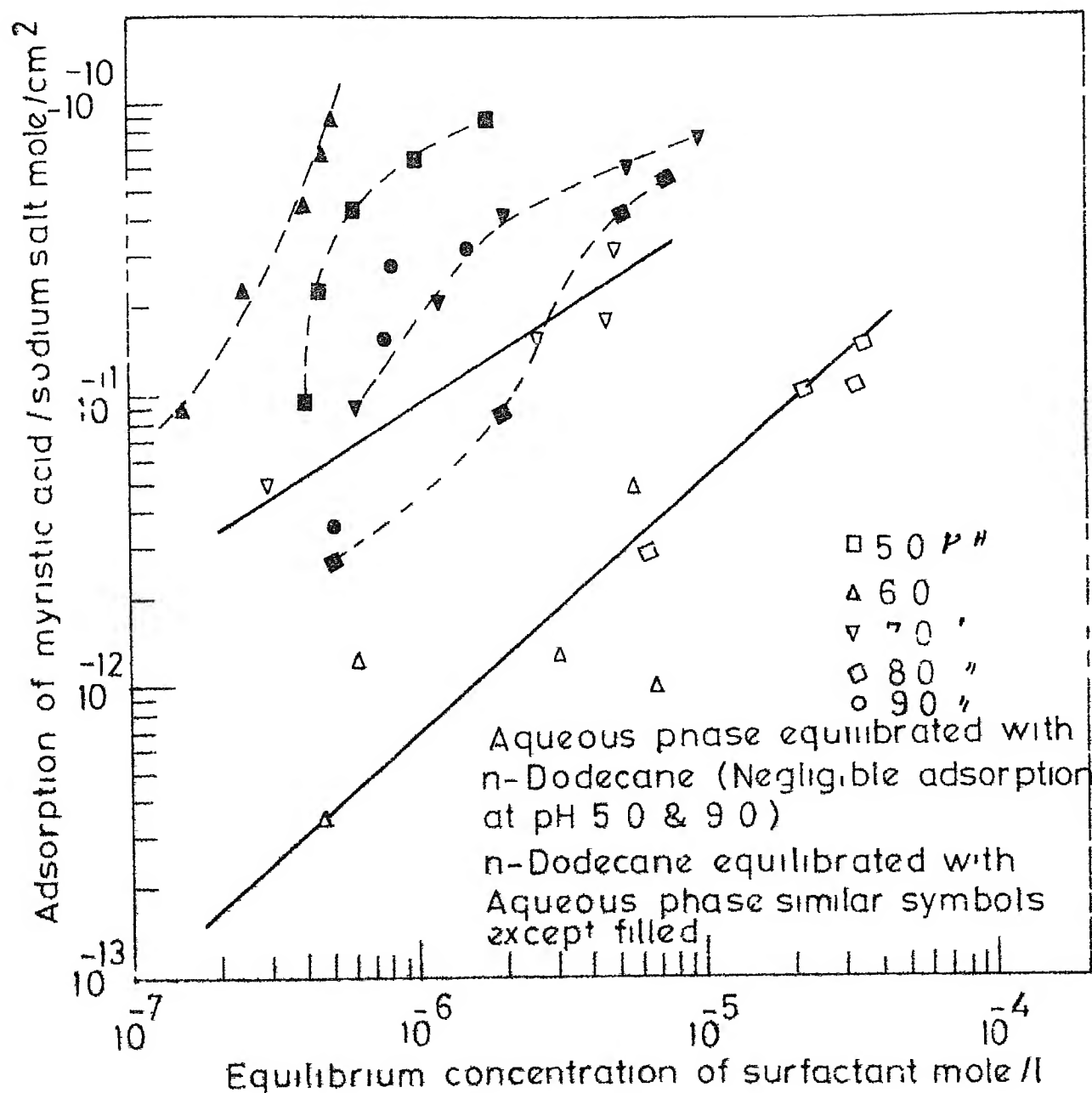
FIG 20   ADSORPTION ISOTHERM OF SODIUM MYRISTATE / MYRISTIC
ACID ON RUTILE FROM ORGANIC AND AQUEOUS PHASE
(From M Tech thesis of A Bhargava[16])
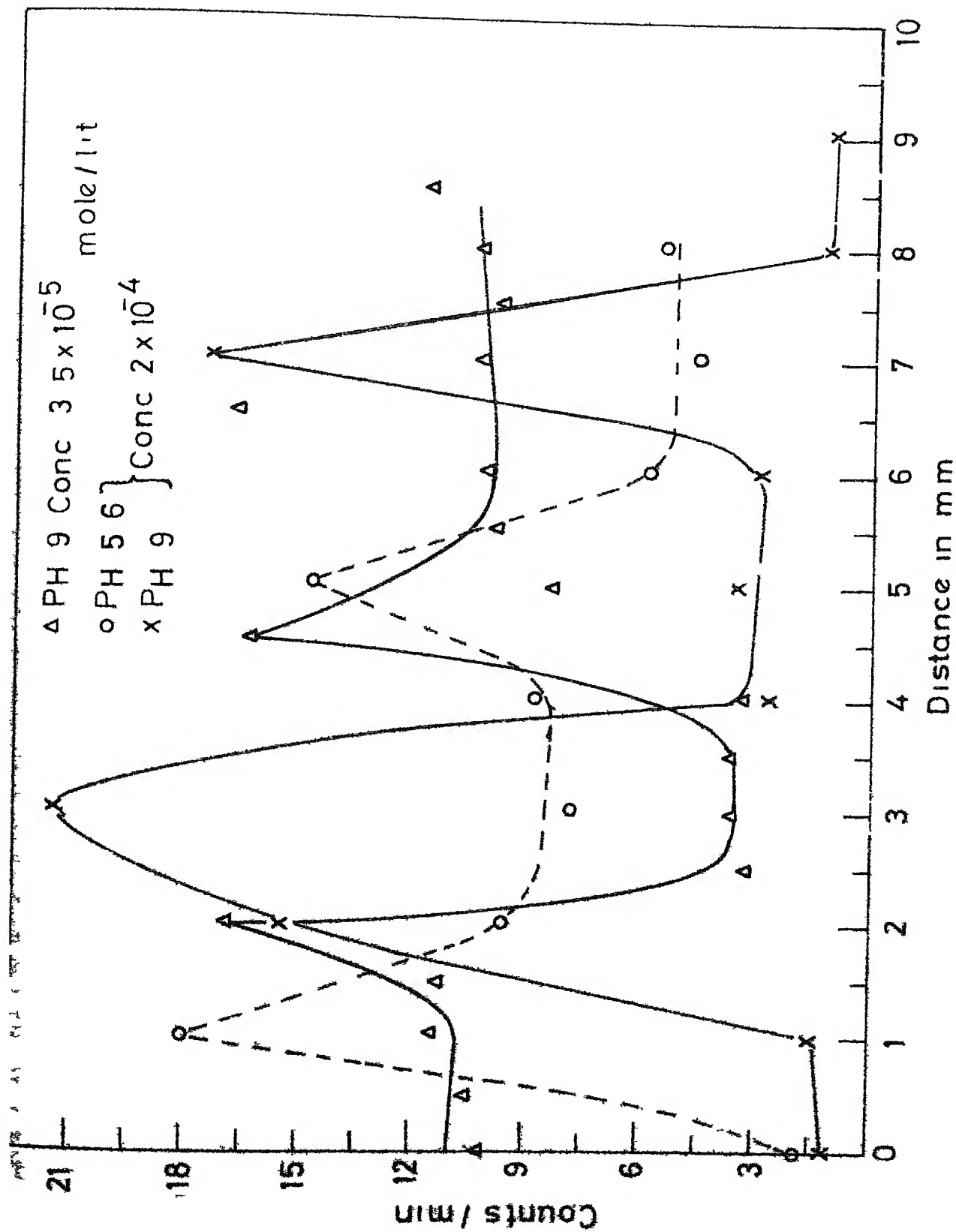
FIG 21 ABSOLUTE COUNT RATE vs DISTANCE ACROSS THREE-PHASE INTERLINE ON CORUNDUM

Collector concentration = 2×10^{-4} mole/lit

x P_H 7
o P_H 8

Counts/min

Distance in mm
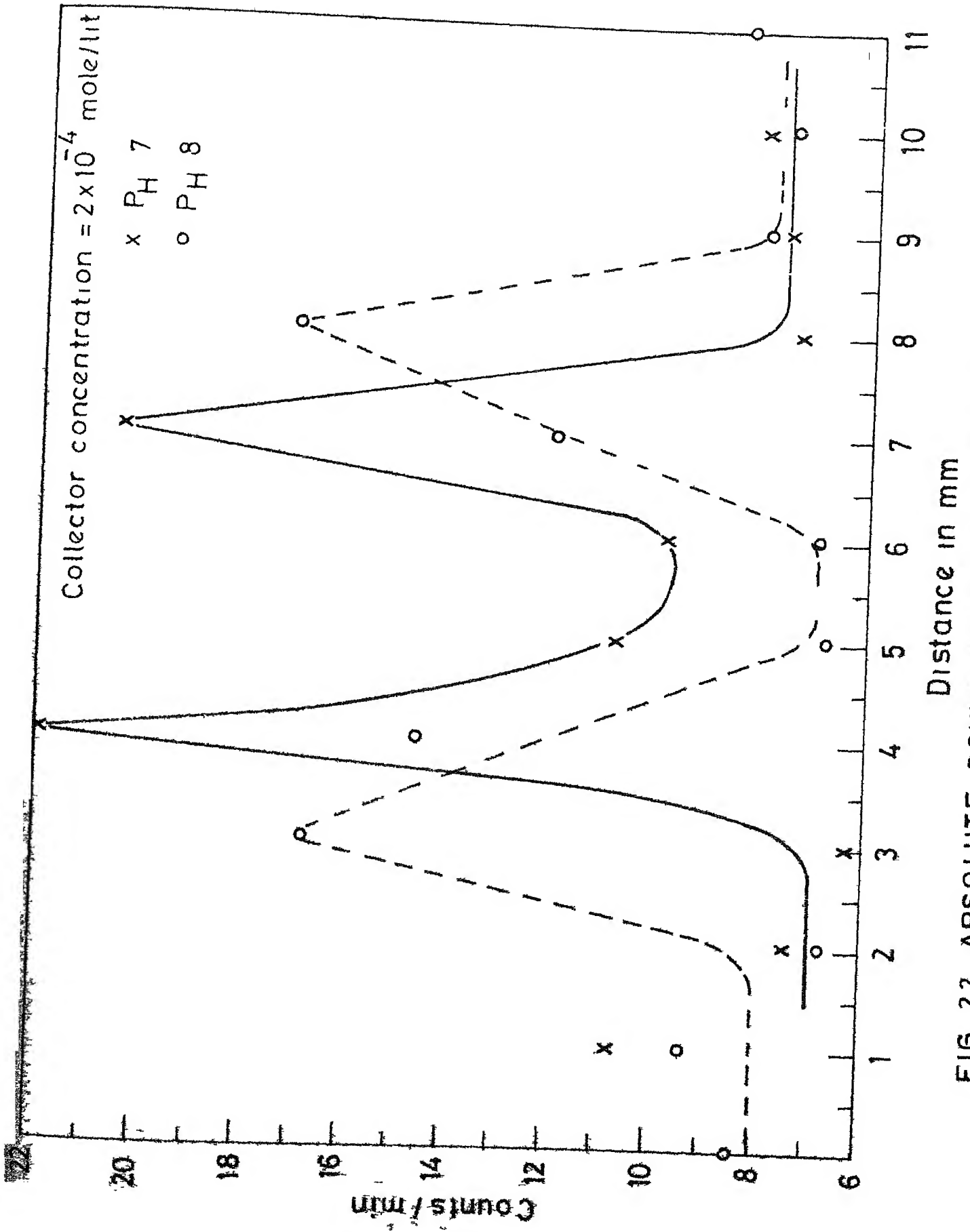
FIG 22 ABSOLUTE COUNT RATE vs DISTANCE ACROSS THREE-PHASE
INTERLINE ON CORUNDUM
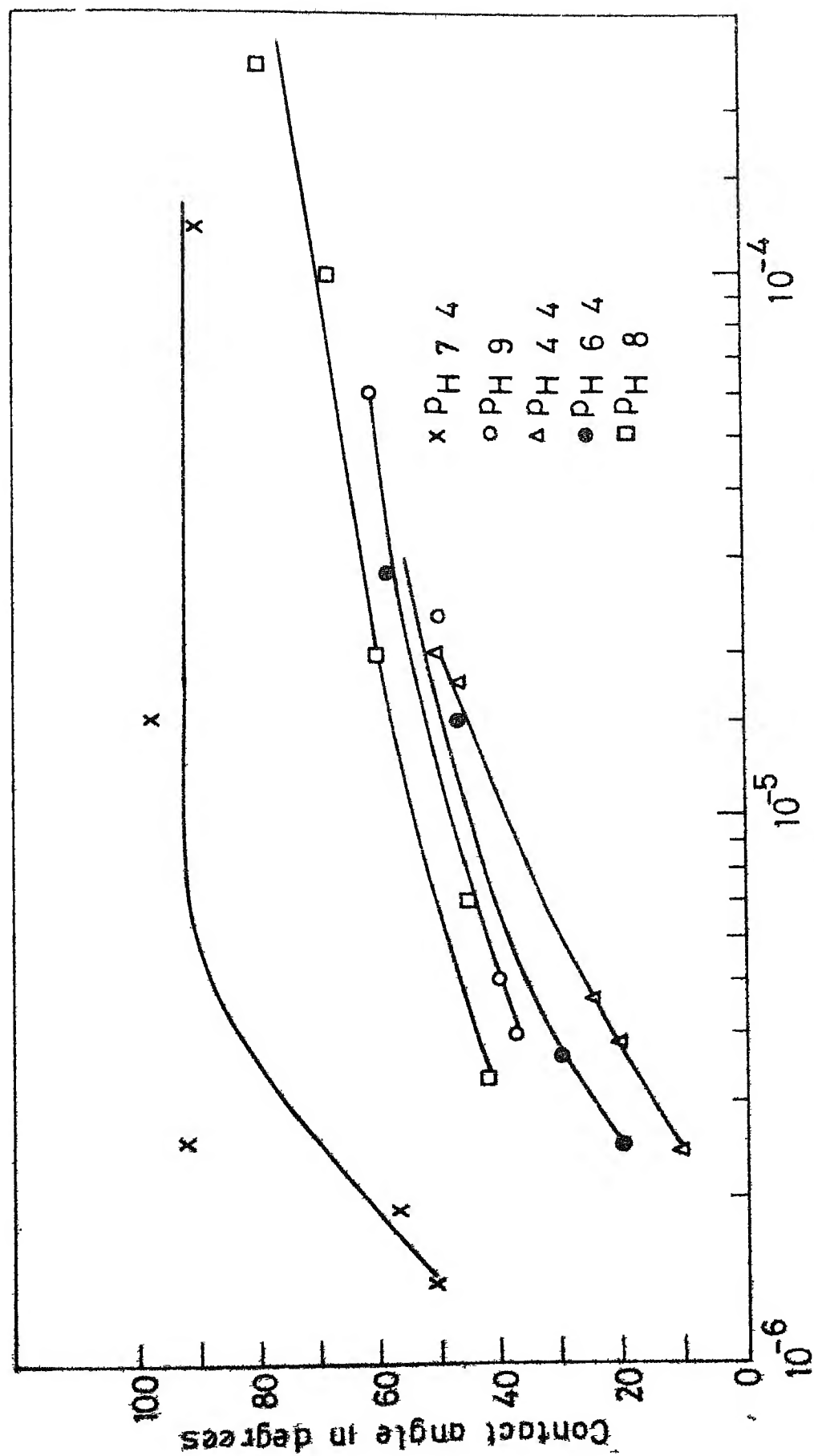
Initial concentration(mole/lit) in the aqueous phase

FIG 23   EFFECT OF SODIUM MYRISTATE CONCENTRATION ON CONTACT ANGLE IN CORUNDUM WATER - DODECANE SYSTEM

4.6 Computation of Interfacial Parameters on Corundum-Water-Dodecane Three-Phase Contact Systems

Presence of sodium myristate/myristic acid as surfactant induces adsorption on the solid-organic liquid, dodecane (SO), solid-water (SW) as well as water-organic liquid (WO) interfaces. Values of Γ_{SO} and Γ_{SW} have been reported earlier in this thesis. Interfacial tension data on water-dodecane-sodium myristate system at different pH and surfactant concentrations have been reported by Bhargava[16] and used in this thesis.

The three interfacial energies γ_{SO}, γ_{SW} and γ_{WO} are related to the contact angle (θ) measured in the aqueous phase. Under equilibrium conditions, Young's equation states.

$$\gamma_{SO} - \gamma_{SW} = \gamma_{WO} \, \cos\theta \tag{1}$$

Finite contact angle of the three-phase system (θ), and increasing hydrophobicity or increasing θ are characterised by decreases in γ_{WO} and $\cos\theta$ and hence of $\gamma_{WO} \, \cos\theta$.

Work of adhesion, W_A is defined as the decrease in surface free energy of the system due to replacement of W/O and S/W interfaces by S/O interface i.e.

$$W_A = \gamma_{WO} + \gamma_{SW} - \gamma_{SO} = \gamma_{WO}(1 - \cos\theta) \tag{2}$$

Table 23 contains (apart from the contact angle data) γ_{WO} values taken from Bhargava's thesis[16] and computed values of γ_{WO} Cosθ and W_A in dynes/cm or ergs/cm^2

The plot in Fig. 24 shows that γ_{WO} Cosθ systematically decreases with increase in surfactant concentration. pH dependence is not severe except in the case of pH 7.4 for which contact angles are larger (vide Fig. 23) and decrease in γ_{WO} Cosθ is maximum at 10^{-5} m/l. surfactant concentration. Fig. 25 also shows maximum θ and work of adhesion at pH around 7.4 when surfactant concentration is 10^{-5} m/l. Adsorption from the aqueous phase (Γ_W) is however maximum around pH 8.0. It may be pointed out that lowering of γ_{WO} was found[16] to be greater when pH was increased from 7.0 to 9.0. Fig. 26 shows maximum recovery of rutile at pH around 9.0 which is larger than the pH values at which θ, Γ_{SW} etc. are maximum[16].

It is difficult to compute changes in the L.H.S. terms in equation (1) i.e. γ_{SO} and γ_{SW} unless the validity of the Gibbs Adsorption Equation is assumed.

$$d\gamma = - s^A dT - \sum \Gamma_i \, d\mu_i \tag{3}$$

where γ is the interfacial energy, s^A, the specific surface entropy, T the temperature, in absolute degrees, Γ_i the surface excess or adsorption in mole/cm^2 and μ

Sodium myristate/myristic acid conc in the aqueous phase (mole/l)
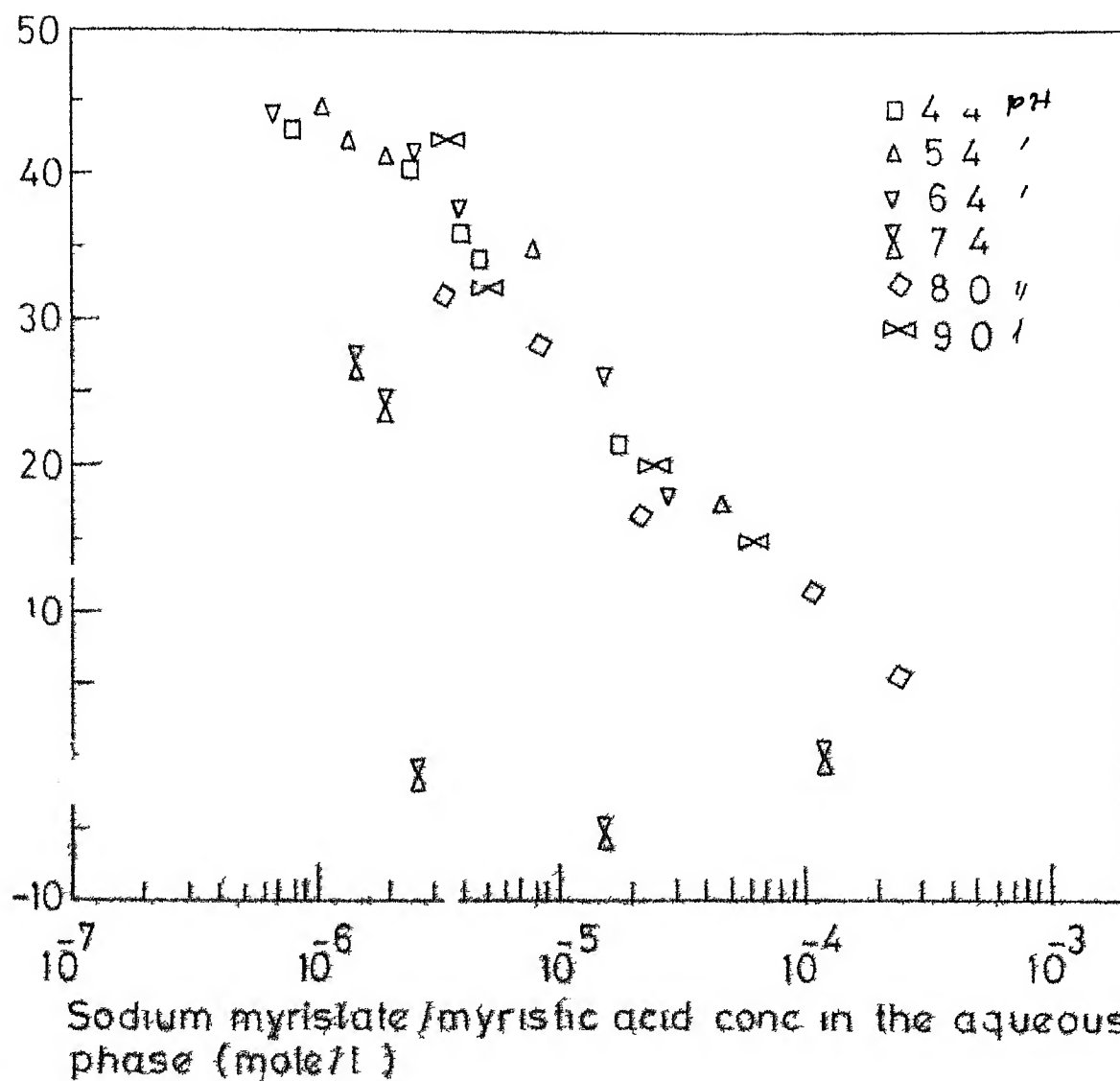
FIG 24 DEPENDENCE OF $Y_{wo}COS \theta$ ON pH AND SURFACTANT CONCENTRATION IN SODIUM MYRISTATE-CORUNDUM SYSTEM
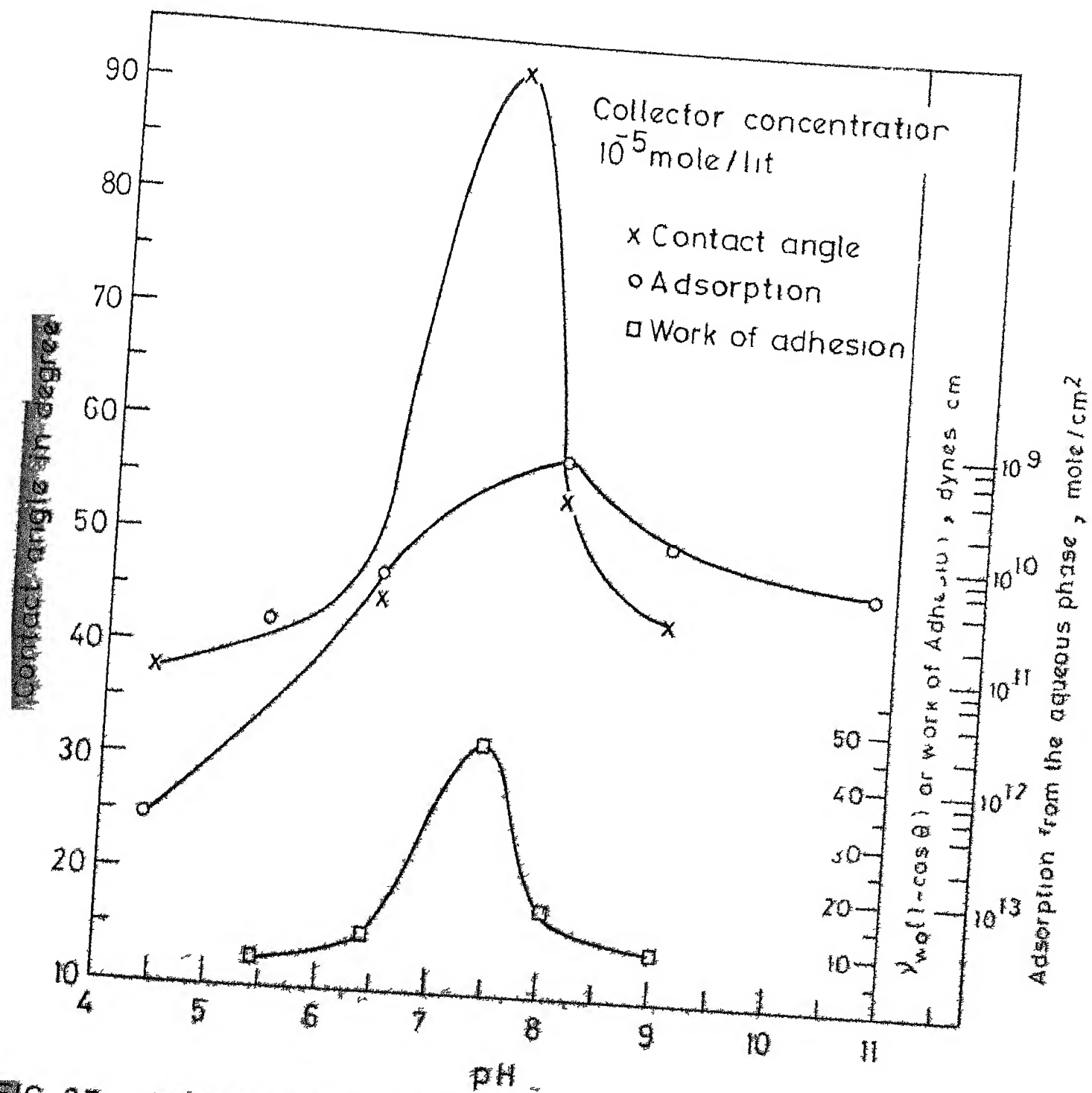
FIG 25 EFFECT OF pH ON CONTACT ANGLE, ADSORPTION FROM THE AQUEOUS PHASE AND WORK OF ADHESION IN CORUNDUM-SODIUM MYRISTATE SYSTEM
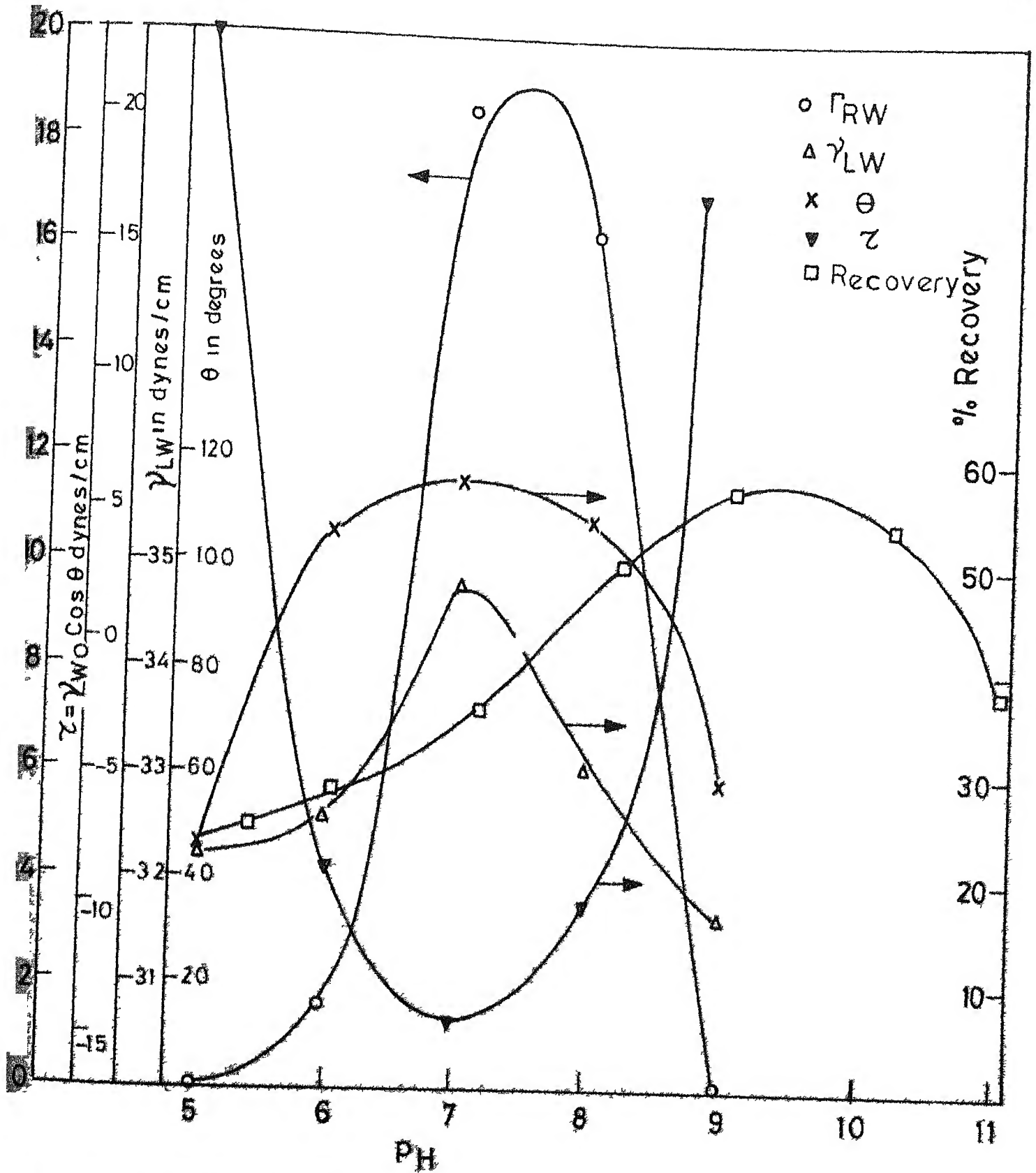
FIG. 6 DEPENDENCE OF $\Gamma_{RW}, \gamma_{W_o}, \theta, \gamma_{W_o} \cos\theta$ & % RECOVERY ON P_H
IN RUTILE - DODECANE WATER - SODIUM MYRISTATE SYSTEM
(All data except recovery values taken from M.Tech thesis
of A Bhargava)

the chemical potential for the ith species. Assuming constant temperature and the presence of only one surfactant species, the previous equation may be re-written as.

$$d\gamma = - \Gamma \, d\mu = - RT \, \Gamma \, d \ln c \qquad (4)$$

c is the bulk concentration equalling activity as an approximation.

If we assume, that the adsorption density

$$\Gamma = K \cdot c^n \qquad (5)$$

where n is the slope in log Γ - log c plot, then equation (4) can be integrated.

$$\Delta\gamma = - \int \Gamma \, d\mu = - 2.303 \, RT \int K \, c^n \, \frac{dc}{c}$$

$$= - 2.303 \times 2.5 \times 10^{10} \cdot K \int c^{n-1} \, dc$$

$$= - 5.75 \times 10^{10} \cdot \frac{K}{n} \, [c^n]_{c_i}^{c_f} \qquad (6)$$

where c_f is the final concentration and c_i the initial value which could be sometimes taken as zero in which case

$$\Delta\gamma = - K' \, c^n \qquad (7)$$

where
$$K' = \frac{5.75 \times 10^{10} \quad K}{n}$$

The data given in Tables 19-21 and Figs. 19-20 have been processed in order to obtain typical values of K, K' and n which are given in Table 24. Typical $\triangle \gamma_{SW}$ and $\triangle \gamma_{SO}$ plots for the corundum system are given in Fig. 27. At very low surfactant concentrations, abstraction of surfactant from the organic phase is almost complete. Adsorption is larger than the extrapolated value. Hence $\triangle \gamma_{SW}$ values are lower than actual.

If Eq. 1 were valid then $(\triangle \gamma_{SO} - \triangle \gamma_{SW})$ would be numerically equal to $\triangle (\gamma_{WO} \cos\theta)$ over a particular range. This has been tested over the range 10^{-7} to 10^{-4} mole/lit. surfactant concentration in the aqueous phase and corresponding equilibrium concentration in the organic phase. Some typical and computed values are given in Table 25.

Interfacial tension data obtained by Bhargava[16] have been used to plot $\gamma - \log c$ plot (Fig. 28) from which tentative value of adsorption density (Γ_{WO}) in the organic liquid-water interface can be computed $\gamma_{WO} \cos\theta$ values are plotted against γ_{WO} in Fig. 29. Typical values of $\frac{d\gamma}{d \log c}$ and $\frac{d(\gamma_{WO} \cos\theta)}{d \gamma_{WO}}$ obtained from the above figures are listed in Table 26.

Significance of all the computed values shall be discussed in the next chapter.

n-Dodecane solution
& Aqueous solution pH 9 0

Aqueous solution pH 6 7,
7 4, 8 0 & 10 8

Aqueous solution
pH 4 4

100

10

1·0

0·1

0 01

10⁻⁷   10⁻⁶   10⁻⁵   10⁻⁴

EQUILIBRIUM CONCENTRATION OF SURFACTANT Mole/Lt
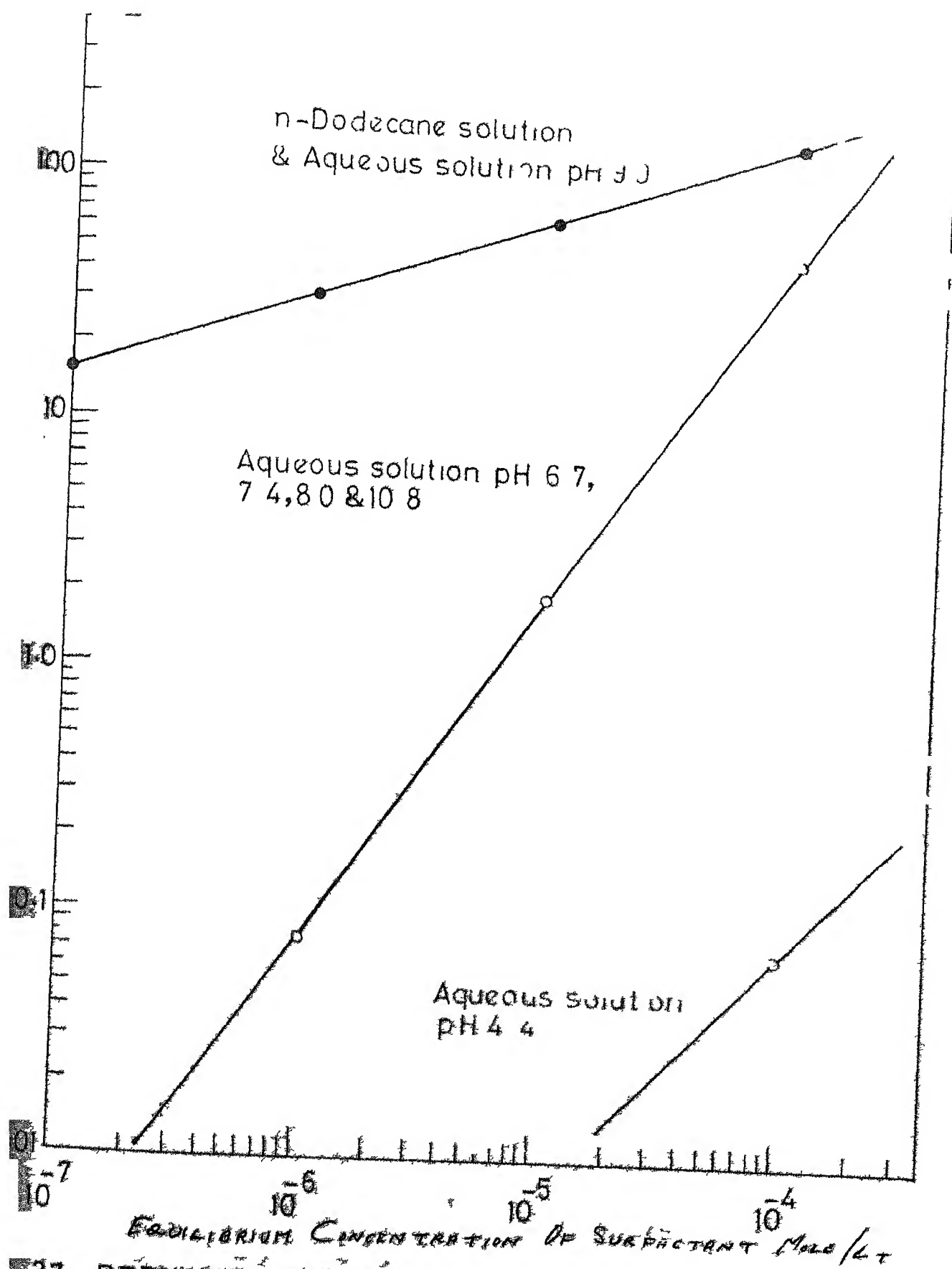
27 REDUCTION OF SURFACE FREE ENERGY OF LIQUID-ALUMINA
INTERFACE AT DIFFERENT EQUILIBRIUM BULK CONCENTRATION
OF SODIUM MYRISTATE/MYRISTIC ACID Based on data in Fig. 19
use of Gibbs adsorption equation,

C, Surfactant concentration mole /lit

Y, Interfacial tension dynes/cm

△ pH 5
○ pH 7
◇ pH 8
□ pH 9
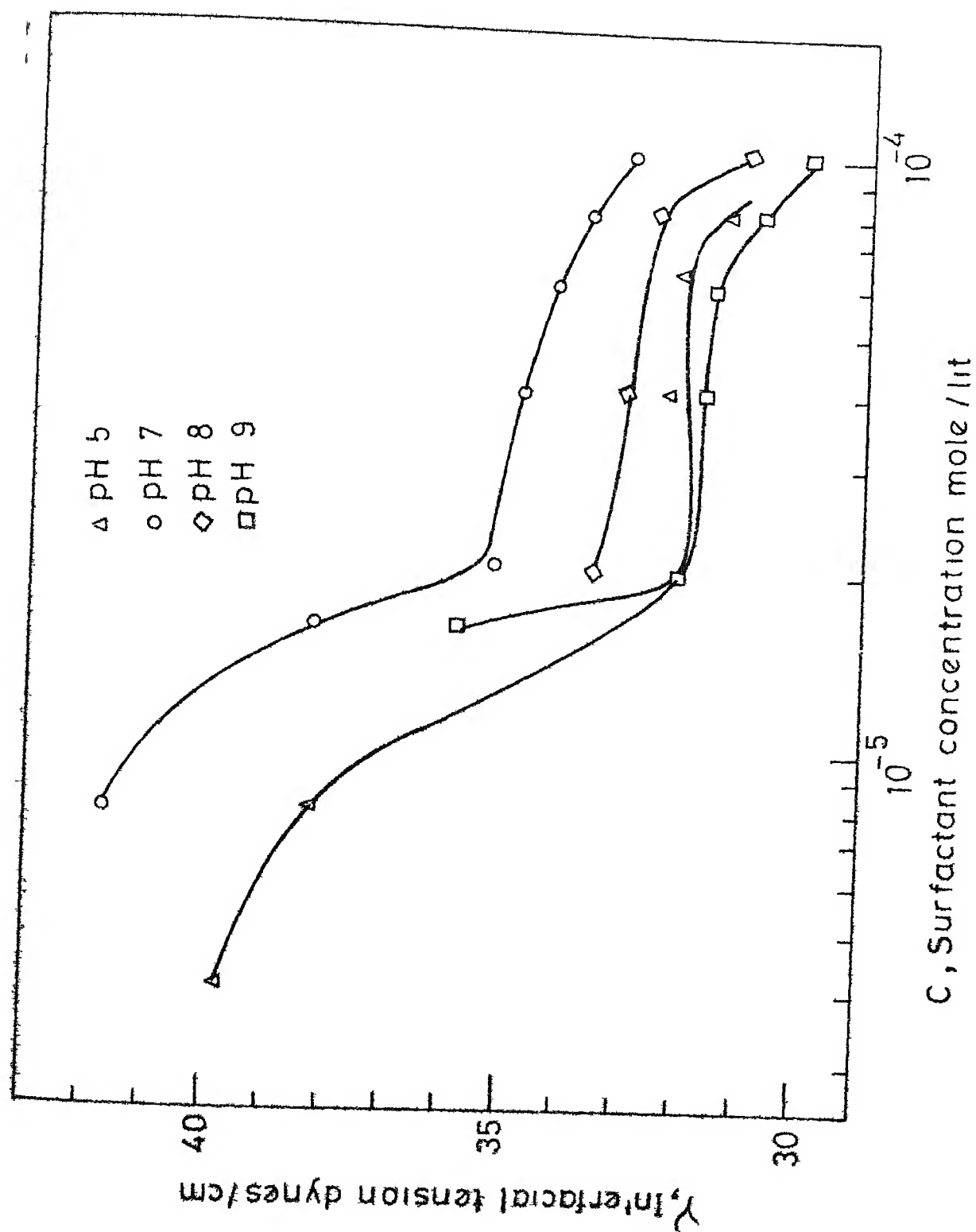
FIG 28 INTERFACIAL TENSION—CONCENTRATION PLOT
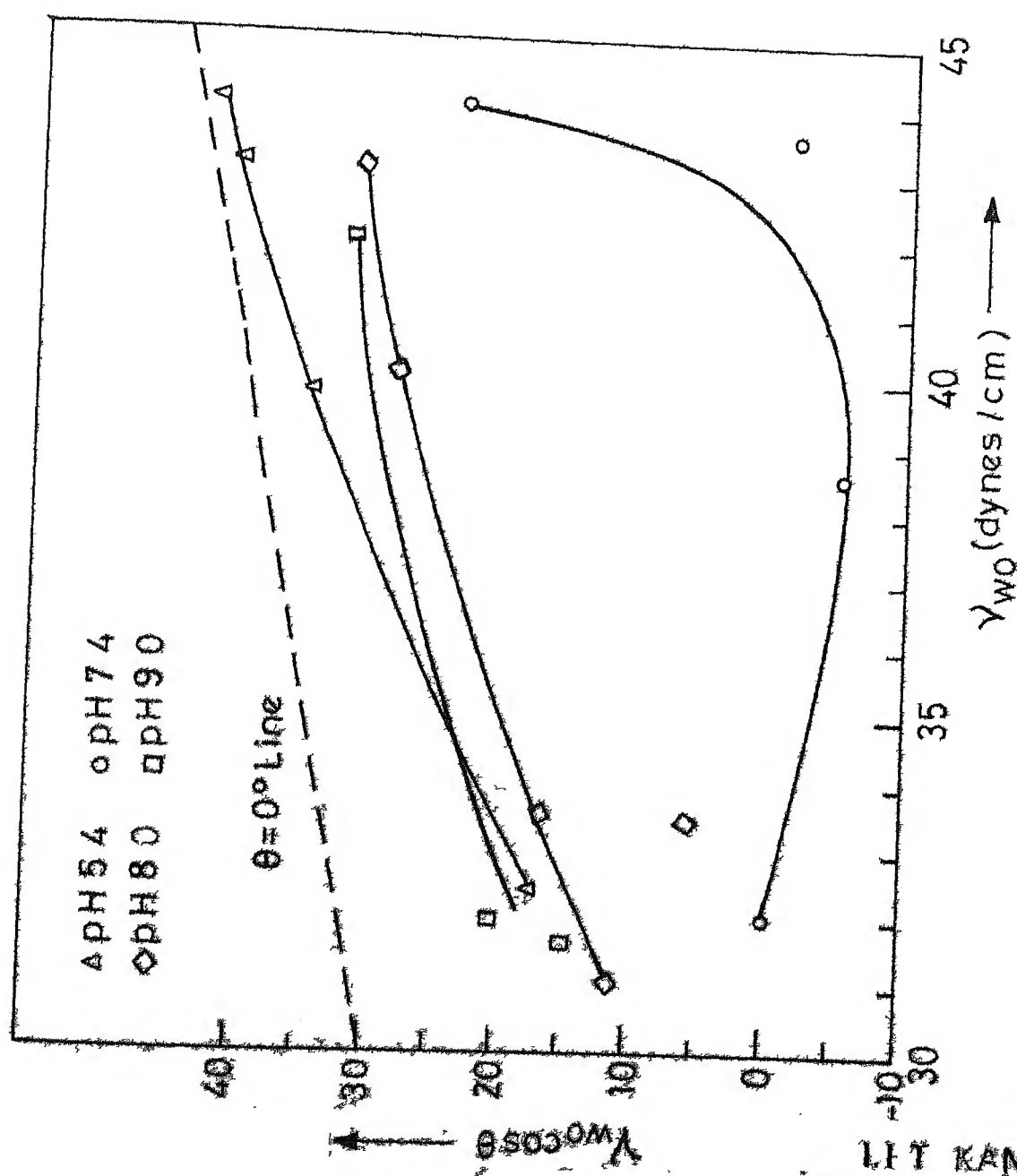
FIG 29 $\gamma_{wo}\cos\theta-\gamma_{wo}$ PLOT FOR DIFFERENT PH VALUES
ON CORUNDUM SYSTEM

CHAPTER 5

DISCUSSION OF RESULTS AND CONCLUSIONS

Recovery of solid particles in the water-organic liquid interface seems to be dependent upon not only (i) the nature of particles (Figs. 9, 11, 13) but also (ii) surfactant concentration (Figs. 10, 11), (iii) pH (Figs. 8, 9, 12 and 13) (iv) particle size and (v) surface treatment (Figs. 8, 10 and 12).

(i) Al_2O_3 and Fe_2O_3 are rendered hydrophobic more easily than TiO_2. It is difficult to separate Al_2O_3 from Fe_2O_3 (Table 17) for which magnitudes of surfactant adsorption are similar (Table 21).

(ii) With increase in collector concentration particularly near its c.m.c. (2.8 - 2.9 x 10^{-4} mole/lit.[16,19]), even coarse Al_2O_3 and TiO_2 (Figs. 10 and 11) are recoverable in greater quantity. This is due to stabler emulsion and more pronounced adsorption of the collector. For Al_2O_3 and Fe_2O_3, pronounced adsorption leads to trapping substantial amount of hydrocarbon — when this oily sludge containing heavy mineral sinks in the aqueous phase lowering the recovery value in the interface. It may be noted in this connection that adsorption density of sodium myristate on Al_2O_3 and Fe_2O_3 at specific pH and collector concentration

are often$_\wedge$ One order of magnitude larger than the corresponding adsorption density on TiO_2 (vide Tables 19, 21 and Figs. 19, 20)

(iii) Figs. 8, 9, 13 and 26 show that recovery of coarse Al_2O_3, Fe_2O_3 and TiO_2 are optimum at some intermediate pH. Some detailed discussions on this point shall be made later in this chapter.

(iv) It is seen that fine particles are more easily recoverable. It is known[6,7] that very good emulsions can be obtained with micron and sub-micron size particles. Thus, at least for the system studied, high pH as well as fine particulate size are distinct factors for stabilising emulsions and hence better recovery.

(v) It is difficult to interpret some of the results given in Figs. 8 and 9 which show that particles are recoverable without any collector. It is known[7] that solids capable of stabilising oil-water emulsions are either inherently wettable partly by oil and partly by water (only low energy solids fall in this category) or are made partly wettable by coating them with a suitable agent. Al_2O_3, Fe_2O_3 and TiO_2 are known as hydrophilic solids. The recovery yields as reported in Figs. 8 and 9 may be due to fine size of the particles, trace surfactant impurities on solids (alumina washed with acetone and

dilute HCl are less recoverable) or trace surfactant impurities in kerosene[8] (which might have remained inspite of alkali treatment and distillation).

Somasundaram and Moudgil found[41] that alumina is flotable in triple distilled water saturated with hydro-carbon gases like methane and butane, and suggested that the hydrocarbon molecules can adsorb at the alumina/solution interface even in the absence of adsorbed collector species. Methane or butane dissolved in sodium dodecyl sulfonate collector solutions was found to increase the flotation of alumina. (Such influences were not observed for hematite or quartz). A similar effect is not unlikely in our system.

The effect of pH on the recovery yield could be a cumulative one of a large number of factors such as variations of: concentrations of surfactant species in the bulk phases; adsorption in the solid-water interface; surface charge on the solid; adsorption on the solid-oil, and oil-water interfaces as well as on the three phase interline affecting contact angle, work of adhesion, lowering of interfacial free energies etc.

Some discussion has been made in Section 4.2 as regards the existence of the surfactant as two possible species - weak or essentially undissociated acid and the

myristate anion, the first being more compatible with the dodecane phase and the second with the aqueous phase. The possibility of the existence of a loose complex between the acid and anion can not be ruled out because if there were only two non-interacting species, then the rigorous treatment given in Section 4.2 demands constancy of 'D', distribution coefficient of myristic acid across the dodecane and water phase irrespective of variation of pH, this is nor borne out in the experimental data (vide Table 18 last column). Association or interaction leading to formation of such a complex is more likely at intermediate pH in which concentrations of the two species in two phases would be substantial.[42] Cockbain and McMullen[27] applied Dalton's law analogue on interfacial tension data for water-decane system and obtained evidence of soap-alcohol interaction.

Interfacial tension measurements have shown[39] the ability of the n-hexadecane and cyclo-hexane oil/water interfaces to support a mixed film of laurate-lauric acid while chloroform did not. Rosane et al. have pointed out earlier[40] that, in micellar solutions of laurate, 1 1 acid soap is formed which is more surface-active than either the neutral soap or lauric acid. The presence of acid-soap at half acidification was confirmed by X-ray data.

Data on adsorption from the aqueous phase
(Tables 19, 21; Figs. 15-20) show very low adsorption
magnitude at low pH such as 4.4 and 5.4 at which the
relative proportions of myristate ions in the aqueous phase
would be low. There are spectroscopic evidences[20,21]
that fatty acid is adsorbed at low pH and the anion
chemically adsorbed at higher pH on oxides like rutile,
ilmenite etc. Some attempts have been made in the past
to attribute optimum interfacial recovery of minerals to
the optimum collector adsorption at the solid-water
interface at some intermediate pH value[12-14,21-22]. In
the present series of study, maximum contact angle and
maximum adsorption of surfactant on corundum took place
at pH 7.5 and 8.0 respectively (Fig. 25)   Complete
recovery of corundum in the water-kerosene interface took
place only when pH exceeded 8.0 (Fig. 8 and 9). Similarly
Fig. 26 shows that for rutile surface, adsorption maxima
is at pH 7.8 and recovery maxima around 9.0. At very high
pH, adsorption of myristate ion is low on account of
competition from OH^- ion to be adsorbed on the solid
surface, and hence the recovery also comes down. This
aspect of competition has been discussed in an earlier
paper[22].

It should also be mentioned that adsorption
from the aqueous phase may not be the only crucial factor.

Shergold and Mellgren's work on hematite-iso-octane-dodecylamine[14] shows that at pH below 5.0, contact angle and recovery values are very low inspite of a reasonably large magnitude of adsorption from the aqueous phase. Evidently, other factors such as adsorption from the organic phase may be crucial as admitted by Shergold and Mellgren[12-14]. Joy and Watson have given evidences[12b,23] that particulate flotation was not uniquely related to the magnitude of adsorption from the aqueous phase. In hematite-dodecylamine system for example, flotation edge line with respect to collector and concentration – pH plot does not correspond to any equal adsorption magnitude curve. Maximum adsorption and recovery have often been claimed to correspond to minimum Zeta potential of the solid surface[9,12-14]. However it has been questioned by Kitchener[14b] whether some 'coincidence' between flotation yield, maximum contact angle and zero Zeta potential could be taken as universal. Iskra and Laskowski have reported[24] that quartz coated with trimethyl chlorosilane floats well with frother alone despite its high Zeta potential. It may be noted here that zero point of charge of alumina is 9 – 9.4,[25] mineral hematite 4.8 – 6.7, synthetic Fe_2O_3 8.6 and rutile TiO_2 5.8 – 6.7.[26]

In a flotation system involving solid-water-gas, it has not been always possible to make direct

measurements regarding surfactant adsorption on the solid-gas interface. Similarly, although several studies have been made on particle recovery in water-organic liquid interfaces, surfactant adsorption on solid-organic liquid interface has hardly been measured. Gaudin and Decker's pioneering work[28] involved adsorption measurement from the organic phase but was not extended to particle recovery.

The present series of study clearly shows (Fig. 19) that adsorption is larger from the organic liquid phase compared to the magnitude of adsorption from the aqueous phase. Above 3×10^{-5} m/l. equilibrium concentration however, and for pH above 7.0, adsorption magnitudes are of similar order, and sometimes the magnitude of adsorption from the aqueous phase is greater. Similar trends have been observed by Gaudin and Decker[28] and by Bhargava[16] (Fig. 20 in this thesis). While comparing the adsorption magnitudes, we must use the distribution coefficient data so that the equilibrium concentration values in the two phases are not necessarily identical. When pH and concentration values are both low, Γ_{SO} is much greater than Γ_{SW}. This satisfies the thermodynamic requirement postulated by De Bruyn, Overbeek and Schuhman[29], and derived on the basis of validity of Gibbs adsorption

and Young's equation. Assuming validity of the two above equations, Smolders derived the relationship[30]

$$\frac{d(\gamma_{WO} \, Cos\Theta)}{d\gamma_{WO}} = \frac{\Gamma_{SO} - \Gamma_{SW}}{\Gamma_{OW}}$$

If De Bruyn's postulate has to be correct the L.H.S. in the above equation has to be positive   This is more or less borne out in the data presented in Fig. 29.   For pH 7.4 and high surfactant concentration however, the slope is negative and Fig. 19 also shows that Γ_{SW} can exceed Γ_{SO} for high pH and surfactant concentration.

It has been suggested earlier in Section 4.6 that with reference to the equation: $\gamma_{SO} - \gamma_{SW} = \gamma_{WO} \, Cos\Theta$, the variations in $\gamma_{WO} \, Cos\Theta$ can be obtained from the experimentally determined values and that changes in γ_{SO} and γ_{SW} can be computed from the adsorption isotherm data assuming Gibbs Adsorption Equation   Equality of the changes in L.H.S. i.e. $(\Delta\gamma_{SO} - \Delta\gamma_{SW})$ with changes in R.H.S. would establish the various thermodynamic postulates Gaudin and Decker reported[28] a qualitative correlation. In our case however (vide Table 25), the correlation is far from satisfactory.   It is significant however that $\Delta\gamma_{SO}$ values are much larger than $\Delta\gamma_{SW}$ values particularly at not-too-high surfactant concentrations, and are of similar order of magnitude as that of $\Delta(\gamma_{OW} \, Cos\Theta)$.

The other basis of correlation of the data
in terms of Gibbs Adsorption and Young's equation is the
equation proposed by Smolder[30,36], given before. Data
in Figs. 28 and 29 and Table 26 show that there is some
qualitative agreement in some cases (e.g. pH 7.4 and 10^{-4}
m/l. aqueous phase concentration). At lower concentration
such as 8×10^{-6} m/l. and pH 7.4, the correlation is very
poor. Γ_{SD} measured is much less than predicted value.
Shergold and Mellgren earlier referred[12,13] to the
unrealistically high value of Γ_{SD} as predicted through
Smolder's equation.

Lack of correlation as mentioned above could be
attributed to the following reasons:

1. Equilibrium may not have been attained.
The phenomenon of hysteresis of contact angle well-
documented by Prof. A.M. Gaudin and his collaborators[28,31]
shows that one could never be sure of the value of equil-
ibrium contact angle.

2. Gibbs adsorption equation may not be valid
particularly when chemisorption is involved as on water-
solid surface for ionic surfactants.

3. Thermodynamic Laplace and Young's equation
do not provide a complete characterisation of equilibrium
with regard to solid-fluid-fluid three phase contact
as shown by De Bruyn et al.[32].

Quantitative confirmation of De Bruyn's postulate[29] and quantitative correlation between contact angle data as measured and as predicted through Gibbs Adsorption Equation and Young's equation have been obtained for three fluid systems such as mercury-gas-water[33]. Attempts for similar correlation in solid-fluid-fluid systems have not yielded positive results so far.

Adsorption measurements across three-phase interline on corundum and rutile has yielded very interesting results. The magnitude of adsorption on the solid-organic liquid interface (Γ_{SO}) relative to Γ_{SW} is much larger in three-phase experiments than the ratio of Γ_{SO}. Γ_{SW} values obtained under two-phase equilibrium conditions (vide Table 22). It has been separately established[34] that the adsorption magnitudes on very fine particles and corresponding coarse particles are of similar magnitude though not identical. It has been also established as shown in Table 22 that rinsing (or lack of it) of the crystal surface after three-phase contact does not alter the ratios substantially. The high value of Γ_{SO} or Γ_{O} can not be attributed to non-attainment of equilibrium. The only plausible reason seems to be transfer of surfactant molecules from the O/W interface to the S/O interface as the three-phase contact gets established. This phenomenon was observed in a flotation system[35].

Furthermore, adsorption at the three-phase interline seems to exceed Γ_{SO} and Γ_{SW} in all cases. Concentration of surfactant at the three-phase interline has been reported earlier[21,37]. Three-phase contact perimeter study made by Viswanathan and Majumdar[38] showed that migration of collector takos place towards the contact perimeter under flotation conditions whereas it does not take place under non-flotation conditions (e.g. in presence of depressor). Table 22 shows that the adsorption density in the interline is in the neighbourhood of the value for a monolayer coverage (6.6×10^{-10} mole/cm^2) and sometimes more. The actual value may indeed be even more because the length of the crystal surface scanned at a time across the three-phase interline (vide Section 3.7) was 0.1 mm. which is likely to be much larger than the thickness of the interline.

To summarise, the studies made in this series indicate that:

1. Al_2O_3, Fe_2O_3 and TiO_2 particles are recoverable in water-kerosene interface in presence of a surfactant such as sodium myristate. The exact magnitude of recovery depends upon size and surface preparation of the particles as well as surfactant concentration and pH.

2. Qualitative relationships exist between the

recovery yield, adsorption magnitudes at different inter-faces (Γ_{SW}, Γ_{SO} and Γ_{OW}).

3. Quantitative correlations between adsorption magnitudes, lowering of interfacial free energies ($\Delta\gamma$) contact angle (Θ), adhesion tension (γ_{OW} $\cos\Theta$), work of adhesion, $\gamma_{OW}(1 - \cos\Theta)$ etc. have been attempted. The correlations are far from satisfactory. Various reasons have been ascribed to explain the lack of good correlation.

4. There are evidences of enhanced adsorption at the (SO) interface mainly from the (OW) interface source during the establishment of three-phase contact. Height-ened adsorption at the three-phase interline to the extent of mono- or multi-molecular coverage has been manifest in most cases. Insofar as these two factors are unaccounted in Young's equation, lack of quantitative correlation as discussed above is not surprising.

5. While the scope of recovery of micron and sub-micron particles in water-organic liquid system is established for three minerals, much more fundamental work is necessary for a basic understanding of the inter-facial process.

REFERENCES

1. Gaudin, A.M., Flotation, 2nd Edition, (New York, McGraw Hill Book Co., Inc., 1957) Chapter 1

2. Gaudin, A.M., Mineral Concentration by Oil Adhesion in the XVth Century, Eng. Mining J., 141 (10), 43-44, 1940

3. McCarroll, S.J., Trans. Soc. of Mining Engrs. of AIME, Trans. 199, 1954, p. 289

4. Flowsheet study - beneficiation of Kaolin clay, Deco Trefoil, 30, No. 3, 1966, 17-18

5. Pickering, Emulsion, J. Chem. Soc., 1907, 2001

6. Hildebrand, J.H., Emulsion type, J. Phys. Chem., 45, 1941, 1303-05

7. Schulman, J.H. and Leja, J., Control of contact angles at the oil-water-solid interfaces-emulsion stabilised by solid particles ($BaSO_4$), Trans. Faraday Soc., 50, 1954, pp. 598-605

8. Grigorov, Yu. N., Sverdlova, N.S., Okatova, I.V., Effect of surfactants on the electrochemical activity of oil-in-water type emulsions stabilised by solid emulsifiers, Elektropoverkhnostnye Yavleniya Dispersnykh Sist. 1972, 64-9 (Russ.) Edited by N.O. Grigorov, 'Nauka', Moscow, U S.S.R. (Chemical Abstract, 79, 1973, 108336j)

9. Lai, R.W.M. and Fuerstenau, D.W., 'Liquid-liquid extraction of ultrafine particles', Trans. Soc. Min. Engrs. of AIME, 241, Dec. 1968, 549-556

10. Zambrana, G.Z., Medina, R.T., Gutierrez, G.B.,and Vargas, R.R., The recovery of minus 10 micron particles of cassiterite, Proceedings of 11th International Mineral Processing Congress, Special Volume issued by Ente Minerario Sardo, Cagliari, April 1975, pp. 449-467

11. Mellgren, O. and Shergold, H.L., Method for Recovering Ultrafine Particles by Extraction with an Organic Phase, Transactions of the Institution of Mining and Metallurgy, Section C, London, 75, 1966, C267-68

12a. H.L. Shergold and Mellgren, O., Concentration of minerals at the oil-water-interface: hematite-iso-octane-water system in the presence of sodium dodecyl sulphate, Transactions of the Institution of Mining and Metallurgy, Section C, 78, Sept. 1969, C121-32

12b. Discussion on the above paper, Trans. IMM., 79, March 1970, pp. C85-88

13. Shergold, H.L. and Mellgren, O., Concentration of minerals at the oil/water interface, Transactions of Soc. Min. Engrs. of AIME, 247, June 1970, pp. 149-159

surfactants with titanium dioxide surfaces, Kolloid Zh. 34, (3), 451-53, 1972

21. Viswanathan, K.V. and Majumdar, K.K., Collector-regulator interactions in the flotation of beach sand minerals under conditions of soap flotation, Transactions of the Indian Institute of Metals, T.P. 697, 26(1), 55-65, Feb 1973

22. Dixit, S.G. and Biswas, A.K., pH dependence of the flotation and adsorption properties of some beach sand minerals, Trans. Soc. Mining Engineers of AIME, 244, 173, 1969   "

23. Watson, D. and Manser, R.M., Some factors affecting the limiting conditions in cationic flotation of silicates, Trans. Inst. of Mining and Metallurgy, Section C, 77, C57-60, 1968

24. Iskra, J. and Laskowski, J., Copper ions in the flotation process: effect of $CuSO_4$ on flotation of methylated quartz, Trans. Inst. of Mining and Metallurgy, Section C, 78, C113-14, 1969

25. Somasundaran, P. and Fuerstenau, D.W., 'J. Phys. Chem., 70, 90-   1966; Modi, H.J. and Fuerstenau, D.W., 'J. Phys. Chem., 61, 640, 1957

26. Parks, G.A. "Chem. Rev., 65, 177, 1965 also A.C.S. Advan. Chem. Ser., 67, 121, 1967

* Mechanisms of alkyl sulfonate adsorption at the alumina-water interface;
' Streaming potential studies on corundum in aqueous solutions of inorganic electrolytes;
" The isoelectric points of solid oxides, solid hydroxides and aqueous hydroxo-complex system.

27. Cockbain, E.G. and McMullen, A.I., 'Adsorbed films
    at oil-water interfaces', Trans. Faraday Society,
    47, 322- , 1951

28. Gaudin, A.M. and Decker, T.G., 'Contact angles and
    adsorption in the system quartz-water-dodecane
    modified by dodecyl ammonium chloride', Journal
    of Colloid and Interface Science, 24, 2, 151-158,
    June 1967

29. De Bruyn, P.L., Overbeek, J.Th.G., and Schuhman,
    R., Jr., Min. Engg. 6, 519, 1954

30. Smolders, C.A. in 'Chemistry, physics and application
    of surface-active substances', (J.Th.G. Overbeek ed.),
    Vol. II, pp. 343-349, Gordon and Breach, London, 1964

31. Gaudin, A.M., Witt, A.F., and Biswas, A.K.,
    'Hysteresis of contact angles in the system organic
    liquid-water-rutile', Trans. Soc. of Mining Engrs.
    of AIME, 229, pp. 1-4, March 1964

32. McLaughlin, B.D. and De Bruyn, P.L., 'Dynamics and
    Thermodynamics of Solid-Fluid-Fluid Three-Phase
    Contact', Journal of Colloid and Interface Science,
    30(1), 21-33, 1969

33. Smolders, C.A., Doctoral Thesis, University of
    Utrecht, Utrecht, The Netherlands, 'Contact angles:
    wetting and de-wetting of mercury part 2. Theory
    of wetting Re c. Trav. Chim. Pays-Bas Belg. T80,
    No. 7, 650-58, July 1961

34. Bansal, V.K. and Biswas, A.K., Collector-frother interaction in the interfaces of a flotation system, Transactions of Institute of Mining and Metallurgy, Section C, June 1975

35. Digre, M. and Sandvik, K.L., Adsorption of amine on quartz through bubble interaction, Trans. Inst. Mining and Metallurgy, 77, C61-C65, June 1968

36. Finch, J.A. and Smith, G.W., Interface adsorption densities in flotation, Journal of Colloid and Interface Science, 44, No. 2, 387-388, August 1973

37. Plaksin, I.N. and Shafeyev, R.Sh., 'On properties of distribution of Xanthate on the surface of sulphide minerals', Journal of Mines, Metals and Fuels, July 1960

38. Viswanathan, K.V. and Majumdar, K.K., The mechanism of collector and regulator interaction in the flotation of beach sand minerals, Journal of Mines, Metals and Fuels, p 106-112, April 1972

39. Cante, C.J., McDermott, J.E., Saleeb, F.Z., and Rosano, H.L., Surface pH from electrokinetic potentials and titration of laurate salts, Journal of Colloid and Interface Science, 50, 1, pp. 1-11, January 1975

40. Rosano, J.L., Briendel, K., Schulman, J.H., and Eydt, A.J., Journal of Colloid and Interfacial

Science, 22, 58, 1966

41. Somasundaran, P. and Moudgil, B.M., 'The effect
of dissolved hydrocarbon gases in surfactant
solutions on froth flotation of minerals',
Journal of Colloid and Interface Science, 47,
No. 2, 290-299, May 1974

42. Stainsby and Alexandar, Trans Faraday Society,
45, 585, 1949.

Table 1

Particle Size Distribution of TiO_2

Size	No. of particles
$\frac{1}{2}$ μ	25
1 μ	39
2 μ	28
3 μ	8

Table 2

Particle Size Distribution of Al_2O_3

Size	No. of particles
$\frac{1}{2}$ μ	3
1 μ	5
2 μ	6
3 μ	8
4 μ	11
5 μ	18
6 μ	21
7 μ	16
8 μ	8
9 μ	4

Table 3

Particle Size Distribution of Fe_2O_3

No. of particles having size $\frac{1}{2}$ μ =	11
No. of particles having size 1 μ =	22
No. of particles having size 2 μ =	40
No. of particles having size 3 μ =	23
No. of particles having size 4 μ =	4

Table 4

Effect of pH on the recovery of Al_2O_3 After Washing with Acetone and Dilute HCl (- 15 μ)

Collector concentration = 0

pH	% recovery
2.5	18.8
3.4	35.0
4.0	36.0
5.0	42.0
7.0	45.0
7.5	100.0 (almost)
8.5	"
10.5	"
11.2	"

Table 5

Effect of pH on the Recovery of Al_2O_3 (Unwashed)

Collector concentration = 0

pH	% recovery
2.3	59.0
3.4	70.0
5.4	77.0
6.3	84.0
7.4	83.0
8.2	94.0
9.5	95.0
10.5	94.0
11.1	90.0

Table 6

Effect of pH on the Recovery of Fe_2O_3 without any Collector

pH	% recovery
2.5	8.0
3.1	8.0
4.0	42.0
5.3	60.0
6.8	90.0
8.4	78.0
9.4	73.0
10.2	72.0
11.5	23.0

Table 7

Effect of pH on the Recovery of TiO_2

Collector concentration = nil

pH	% recovery
2.5	3.7
4.5	7.8
5.4	11.0
6.3	10.0
7.0	15.0
8.2	19.5
9.8	22.0
10.3	21.5
11.5	17.0

Table 8

Effect of Collector Concentration on Recovery of Al_2O_3

pH = 7.5

Collector concentration moles/lit	% recovery
0	100 (almost)
1×10^{-5}	"
1×10^{-4}	"
2×10^{-4}	"
5×10^{-4}	"
8×10^{-4}	"
10^{-3}	"

Table 9

Effect of Collector Concentration on the Recovery of Al_2O_3 (Unwashed)

Collector concentration moles/lit	recovery
0	94
10^{-5}	96
10^{-4}	97
2×10^{-4}	96
3×10^{-4}	85
4×10^{-4}	80
5×10^{-4}	85

Table 10

Effect of Collector Concentration on the Recovery of Fe_2O_3

Collector concentration moles/lit	% recovery
0	87
10^{-5}	86
10^{-4}	90
2×10^{-4}	93
3×10^{-4}	80
4×10^{-4}	60
5×10^{-4}	38
10^{-3}	26

Table 11

Effect of Collector Concentration on the

Recovery of TiO_2 at 7 6 pH

Collector concentration moles/lit	% recovery
10^{-5}	20
10^{-4}	22
2×10^{-4}	25
4×10^{-4}	35
6×10^{-4}	47
8×10^{-4}	43
10^{-3}	40

Table 12

Effect of pH on Recovery of Washed Alumina

Collector concentration = 2×10^{-4} mol/lit

pH	$^o/_o$ recovery
2.5	100 (almost)
3.5	"
4.5	"
6.0	"
7.5	"
8.5	"
9.5	"
10.0	"
11.0	"

Table 13

Effect of pH on the Recovery of Al_2O_3 (Unwashed)

Collector concentration = 2×10^{-4} mol/lit.

pH	% recovery
2.0	62.0
3.2	67.0
4.1	90.0
5.5	93.0
6.2	92.0
7.6	93.0
8.5	92.0
9.5	92.5
10.4	91.0
11.5	88.0

Table 14

Effect of pH on the Recovery of Fe_2O_3 at 2×10^{-4} moles/lit Collector Concentration

pH	$^0/_0$ recovery
2.0	85
2.8	86
4.2	88
5.8	91
7.4	98
8.4	97
9.5	97
10.4	91
11.5	88

Table 15

Effect of pH on the Recovery of TiO_2

Collector concentration $= 0.4 \times 10^{-4}$ mole/lit.

pH	% recovery
2.0	21
2.5	22
3.2	18
4.2	23
5.2	25
6.0	28
7.1	36
8.2	50
9.0	57
10.2	54
11.0	37

Table 16

Effect of pH on the Recovery of TiO_2

Collector concentration $= 2 \times 10^{-4}$ mole/lit.

pH	% recovery
2.5	32
4.5	45
5.5	40
7.5	42
8.5	58
9.5	60
10.5	83
11.5	69
11.7	70

Table-17

Separation of Fe$_2$O$_3$ from Al$_2$O$_3$ through Liquid-Liquid Interfacial Recovery

Expt. No.	pH	Collector concn. mole/lit	Total wt (g) recovered out of 1 g. ie 0.5 Fe$_2$O$_3$ 0.5 Al$_2$O$_3$	Assay of product per cent Fe$_2$O$_3$	Per cent recovery of Fe$_2$O$_3$	Per cent recovery of Al$_2$O$_3$	Comments
1	2.4	0	0.42	65.6	54.8 (8)	29.2 (19)	Compared to the pure system situations, recovery values are higher
2	2.8	0	0.54	34.5	38.4 (8)	68.6 (20)	"
3	2.8	4x10^{-5}	0.44	48.0	42.4	45.6	Emulsion is not appreciable
4	2.1	10^{-4}	0.33	68.0	45.2 (40)	10.6	Both Fe$_2$O$_3$ and Al$_2$O$_3$ are collected at the interface; Fe$_2$O$_3$ at the top layer
5	1.9	2x10^{-4}	0.38	63.0	48.0 (85)	28.0 (62)	Similar situation as above
6	2.7	2x10^{-4}	0.56	24.0	27.0 (85)	83.0 (66)	Al$_2$O$_3$ and Fe$_2$O$_3$ are collected simultaneously. More of Al$_2$O$_3$ in the interface
7	7.5	10^{-4}	0.85	59.0	100.0 (90)	70.0 (87)	There is an emulsion layer; Fe$_2$O$_3$ at the top and Al$_2$O$_3$ at the bottom

Bracketted figures indicate the p.c. recovery values in the pure systems.

Table 17 continued.

Expt. No.	pH	Collector concn. mole/lit	Total wt (g) recovered out of 1 g. 0.5g Fe₂O₃ 0.5g Al₂O₃	Assay or product of per cent Fe₂O₃ Al₂O₃	Per cent recovery of Fe₂O₃	Per cent recovery of Al₂O₃	Comments
8	10.9	10^{-4}	0.65	61.0	79.2 (80)	50.4 -	Emulsion is stabler than that in the previous experiment
9	7.6	2×10^{-4}	0.6	65.0	78.0 (93)	42.0 (96)	No sludge formation is observed as in pure Fe₂O₃ system. There is a kinetic effect, Fe₂O₃ getting collected much earlier than Al₂O₃
10	7.6	5×10^{-4}	0.65	60.0	78.0 (40)	52.0 (85)	Observations are similar as above.

Table 18

Variation of 'K$_D$' and 'D' with pH

$$K_a = \frac{K_h}{K_w} \simeq \frac{10^{-9}}{10^{-14}} \simeq 10^5$$

pH	H$^+$	K$_a$H$^+$	K$_d$	D = K$_d[(1+K_aH^+)/K_aH^+]$
4.4	$10^{-4.4}$	4.0	11.46	14.32
5.4	$10^{-5.4}$	0.4	6.71	23.50
6.4	$10^{-6.4}$	4×10^{-2}	5.15	1.29×10^2
7.4	$10^{-7.4}$	4×10^{-3}	3.22	8.05×10^2
8.0	$10^{-8.0}$	10^{-3}	0.8775	8.8×10^2
9.0	$10^{-9.0}$	10^{-4}	0.308	3.1×10^3
10.8	$10^{-10.8}$	1.6×10^{-6}	0.151	9×10^4

Table 19

Absorption from Aqueous Solution on Al_2O_3 Powder

Sl. No.	pH	Counts per minute before absorption	Initial concen. moles/lit $x10^5$	Count rate/min after absorption	Concen. of soln. after absorption $x10^5$	Amount absorbed in moles/gm $x10^7$	$\Gamma^* \quad \Gamma(=\Gamma^*/3. \quad x10^3)$ moles/cm^2 $x10^9$
1	10.8	830.0	33.25	151.0	6.0	27.25	0.908
2		356.0	14.25	106.8	4.25	10.00	0.34
3		158.4	6.5	58.6	2.5	4.00	0.133
4		58.9	2.5	24.24	1.0	1.5	0.05
5		30.92	1.5	16.92	0.845	0.655	0.022
1	9.0	–	89.5	–	58.5	31.0	1.03
2		454.2	17.0	93.24	3.5	13.5	0.45
3		207.12	7.75	72.48	2.75	5.0	0.17
4		47.4	1.74	25.56	0.105	1.63	0.054
5		39.6	1.5	13.68	0.051	1.449	0.048
6		30.76	1.16	4.44	0.0165	0.995	0.033
1	8.0	–	76.0	–	20.4	55.6	1.85
2		2067.72	24.8	545.52	6.55	18.25	0.608
3		879.6	10.57	252.24	3.35	7.22	0.241
4		176.16	2.11	56.28	0.675	1.435	0.048
5		75.6	0.81	47.52	0.575	0.235	0.0075
6		27.48	0.331	12.72	0.153	0.178	0.0059
1	7.4	402.0	12.0	172.00	5.0	7.0	0.233
2		52.0	1.5	37.68	1.12	0.38	0.0127
3		8.64	0.24	4.8	0.13	0.11	0.0037
4		6.48	0.194	3.24	0.0875	0.1065	0.00355
5		3.48	0.0945	0.0	0.0	0.0945	0.00315
1	6.4	261.6	2.8	116.16	1.21	1.59	0.053
2		125.0	1.3	56.04	0.585	0.715	0.024
3		35.28	0.365	17.04	0.177	0.188	0.0063
4		24.6	0.257	8.04	0.083	0.174	0.0055
5		7.8	0.081	5.52	0.0575	0.024	0.0008

Table 19 continued.

Sl. No.	pH	Counts per minute before absorption	Initial concen. moles/lit $\times 10^5$	Count rate/min after absorption	Concen. of soln. after absorption $\times 10^5$	Amount Γ^* absorbed in moles/gm $\times 10^7$	$\Gamma(=\Gamma^*/3.0\times10)$ moles/cm^2 $\times 10^9$
1	5.4	288.6	3.8	153.6	2.0	1.8	0.06
2		101.0	1.33	71.3	0.89	0.44	0.0147
3		14.64	0.183	11.76	0.147	0.036	0.0012
4		10.56	0.132	8.52	0.106	0.026	0.00087
5		5.76	0.076	4.08	0.0535	0.023	0.00077
1	4.4	135.48	2.5	133.92	2.48	0.02	0.00068
2		95.4	1.75	94.88	1.748	0.01	0.00034
3		25.32	0.462	24.72	0.457	0.005	0.00017
4		20.76	0.38	20.4	0.337	0.003	0.0001
5		6.6	0.122	6.6	0.122	0.0	-
6		3.84	0.071	3.96	0.079	0.0	-

Table 20

Adsorption from Organic Phase (Dodecane)

Sl.	pH	Counts/min before adsorption	Initial concen. moles/lit $\times 10^5$	Counts/min after equilibration with solid	Corresponding amount in moles/lit $\times 10^5$	Γ^* Amount adsorbed in moles/g. $\times 10^6$	$\Gamma^* = (\Gamma^*/3 \times 10^3)$ mole/cm^2 $\times 10^9$
1	10.8	60.00	2.5	14.64	0.05	0.245	0.08
2		30.22	1.250	11.64	0.375	0.0875	0.029
3		20.6	0.75	8.04	0.25	0.05	0.017
4		14.6	0.53	5.64	0.22	0.03	0.01
5		9.0	0.3	4.8	0.19	0.011	0.004
1	9.0	155.4	6.0	5.76	0.217	0.5783	0.19
2		60.8	2.3	0.0	0.0	0.23	0.073
3		16.8	0.5	0.0	0.0	0.05	−
4		15.24	0.45	0.0	0.0	0.045	−
5		10.56	0.35	0.0	0.0	0.035	
1	8.0	1289.28	15.6	10.8	0.13	1.547	0.51⁶
2		751.92	9.1	5.88	0.0705	0.903	0.30⁷
3		152.5	1.8	0.0	0.0	0.1805	0.06
4		65.04	0.785	0.0	0.0	0.0785	−
5		25.0	0.301	0.0	0.0	0.0301	−
1	7.4	1080.48	32.2	30.0	0.816	3.1384	1.046
2		165.0	4.9	17.28	0.47	0.443	0.148
3		25.68	0.7	0.0	0.0	0.07	0.0023
4		25.44	0.69	0.0	0.0	0.069	−
5		10.88	0.295	0.0	0.0	0.0295	−
1	6.4	1346.0	14.0	448.44	4.675	0.9325	0.31
2		617.2	6.35	194.76	2.01	0.434	0.145
3		182.5	1.9	17.28	0.177	0.1723	0 057
4		129.5	1.35	9.6	0.1	0.125	0.042
5		43.2	0.45	3.0	0.0312	0.04188	0.014

Table 20 continued.

Sl. No.	pH	Counts/min before adsorption	Initial concen. moles/lit $\times 10^5$	Counts/min after equilibriation with solid	Corresponding amount in moles/lit $\times 10^5$	Γ^* Amount adsorbed in moles/g. $\times 10^6$	$\Gamma = (\Gamma^*/3\times10^3)$ mole/cm^2 $\times 10^9$
1	5.4	1950.0	25.65	1479.0	19.4	0.625	0.208
2		704.04	9.25	385.08	5.075	0.4175	0.14
3		92.7	1.22	50.52	0.665	0.0555	0.018
4		64.2	0.845	20.4	0.268	0.0577	0.019
5		39.88	0.515	0.0	0.0	0.0515	0.017
1	4.4	1385.00	25.6	103.68	2.0	2.36	0.79
2		1006.8	18.65	78.0	1.44	1.721	0.57
3		365.4	6.7	16.08	0.2975	0.64025	0.21
4		257.4	4.75	11.88	0.2	0.455	0.152
5		64.8	1.18	7.68	0.142	0.1038	0.034
6		43.2	0.8	2.04	0.037	0.0763	0.025

Table 21

Adsorption of Sod. myristate on Al_2O_3 from Water at High Concentration

Sl. No.	pH	Counts per 500 sec before adsorption	Counts per min. before adsorption	Initial concentration (before adsorption)	Counts per 500 sec after adsorption	Counts per min after adsorption	Concentration after adsorption	Amount adsorbed per gram
1	10	56272	$(56272-540) \frac{12}{\times 100}$ 6687.84	0.98×10^{-3}	45206	5371.92	7.88×10^{-4}	1.92×10^{-6}
2	9	51385	6101.4	0.895×10^{-3}	34888	4121.76	0.585×10^{-3}	3.1×10^{-6}
3	8	43845	5196.6	0.76×10^{-3}	12433	1427.16	2.04×10^{-4}	5.56×10^{-6}
4	7	28041	3420.12	0.485×10^{-3}	10651	1213.32	1.79×10^{-4}	3.1×10^{-6}

Adsorption of Sod. myristate on Fe_2O_3 from Water at High Concentration

Sl. No.	pH	Counts per 500 sec before adsorption	Counts per min. before adsorption	Initial concentration (before adsorption)	Counts per 500 sec after adsorption	Counts per min after adsorption	Concentration after adsorption	Amount adsorbed per gram
1	10	56272	6687.84	0.98×10^{-3}	12299	1311.08	1.75×10^{-4}	8.05×10^{-6}
2	9	51385	6101.40	0.895×10^{-3}	6531	718.92	1.055×10^{-4}	7.895×10^{-6}
3	8	43845	5196.6	0.76×10^{-3}	5587	605.64	8.85×10^{-5}	6.715×10^{-6}
4	7	28041	3420.12	0.485×10^{-3}	4680	496.80	7.3×10^{-3}	4.12×10^{-6}

Table 22

Adsorption Measurements Across Three Phase Interline on Corundum

(Legand: R - Surface rinsed after three phase contact; NR - not rinsed; W - stands for water or aqueous phase; o - for organic or dodecane phase; and i - for three-phase interline)

Expt. No.	R or NR	pH	C_o concentration of surfactant mole/l.	Corresponding C_o	Relative adsorption density magnitudes $\Gamma_w : \Gamma_o : \Gamma_i$ in counts per minute as well as normalised	$\Gamma_w : \Gamma_o$ from equilibrium adsorption data (Fig. 19) in moles/cm² and also normalised	Computed Γ_i in mole/cm²
1	R	7.0	2×10^{-4}	7.8×10^{-4}	$7.30 : 9.7 : 21.25$ $1 : 1.33 : 2.94$	$3 \times 10^{-9} : 6 \times 10^{-10}$ $1 : 0.2$	8.8×10^{-9}
2	NR	7.0	1.79×10^{-4}	7.0×10^{-4}	$6.25 : 11.09 : 20.88$ $1 : 1.77 : 3.34$	$2.5 \times 10^{-9} : 5 \times 10^{-10}$ $1 . 0 . 2$	8.35×10^{-9}
3	R	8.0	2×10^{-4}	1.6×10^{-4}	$7.9.7.0.17.0$ $1 : 0.885 . 2.15$	$3 \times 10^{-9} : 3.5 \times 10^{-10}$ $1 : 0.117$	6.45×10^{-9}
4	NR	8.0	2×10^{-4}	1.6×10^{-4}	$10.25.8.91 : 19.72$ $1 : 0.691 : 1.924$	As Above	5.77×10^{-9}
5	R	9.0	3.5×10^{-5}	1.05×10^{-5}	$10.51 : 3.45 : 17.10$ $1.0.3 : 1.62$	$2.1 \times 10^{-10} : 1.4 \times 10^{-10}$ $1 : 0.66$	3.4×10^{-10} Data obtained from severe extrapolation

Table 22 continued

Expt. No.	R or NR	pH	C_W concentration of surfactant mole/l.	Corresponding C_o	Relative adsorption density magnitudes $\Gamma_W:\Gamma_o:\Gamma_i$ in counts per minute as well as normalised	$\Gamma_W:\Gamma_o$ from equilibrium adsorption data (Fig. 19) in moles/cm2 and also normalised	Computed Γ_i in mole/cm2
6	NR	9.0	3.5×10^{-5}	1.05×10^{-5}	14.04:4.43:20.46 1:0.316:1.46	$2.1\times10^{-10}:1.4\times10^{-10}$ 1:0.66	3.06×10^{-10}
7	R	10.8	6.0×10^{-5}	9×10^{-6}	19.11:13.68.27.58 1:0.72:1.44	$6\times10^{-10}:1.3\times10^{-10}$ 1.0.22	8.64×10^{-10}
8	NR	10.8	6.0×10^{-5}	9×10^{-6}	21.27:15.35:29.7 1 0.72:1.39	$6\times10^{-10}:1.3\times10^{-10}$ 1:0.22	8.34×10^{-10}

Typical Data for Rutile[16]

Expt. No.	R or NR	pH	C_W concentration of surfactant mole/l.	Corresponding C_o	Relative adsorption density magnitudes $\Gamma_W:\Gamma_o:\Gamma_i$ in counts per minute as well as normalised	$\Gamma_W:\Gamma_o$ from equilibrium adsorption data (Fig. 19) in moles/cm2 and also normalised	Computed Γ_i in mole/cm2
1	R	7.0	2×10^{-5}	8×10^{-5}	1:4.5:8.6	$6.0\times10^{-11}:2.0\times10^{-10}$ 1:3.33	5.16×10^{-10}
2	R	7.0	1×10^{-4}	4×10^{-4}	1:2.95:4.9	$1.7\times10^{-10}:4.2\times10^{-10}$ 1:2.47	8.33×10^{-10}

Table 23

Effect of pH on Contact Angle (Θ), γ_{WL} etc. in the Al_2O_3-Water-Dodecane-Sodium Myristate System

Sl. No.	pH	Concentration moles/lit.$\times 10^5$ C_W	C_o	Contact angle (Θ) in/degrees	γ_{WO} dynes	$\gamma_{WO}\cos\Theta$ per	W_A^* or $\gamma_{WO}(1-\cos\Theta)$ cm
1	4.4	2.5	21.0	50	31.4	20.1	11.3
2		1.75	15.0	47	31.6	21.5	10.1
3		0.46	3.9	25	38.1	34.3	3.8
4		0.38	3.2	20	38.3	36.0	2.3
5		0.24	2.0	10	41.5	40.7	0.8
6		0.075	0.64	–	43.2	43.2	0.0
1	5.4	4.56	26.5	58	32.4	17.2	15.2
2		0.75	5.0	25	38.8	34.9	3.9
3		0.18	1.2	18	43.1	40.9	2.2
4		0.13	0.88	17	44.0	42.2	1.8
5		0.10	0.68	–	44.5	44.5	0.0
1	6.4	2.8	14.0	58	33.9	18.0	15.9
2		1.5	7.5	45	36.9	26.2	10.7
3		0.37	1.8	30	43.0	37.4	5.6
4		.0.26	1.3	20	44.0	41.4	2.6
5		0.06	0.31	–	44.2	44.2	0.0
1	7.4	12.0	37.0	90	32.0	0.00	32.0
2		1.5	4.7	98	38.6	-5.4	44.0
3		0.25	0.78	92	43.6	-1.3	44.9
4		0.19	0.59	57	44.0	23.8	20.2
5		0.14	0.43	52	44.0	27.3	16.7
1	8.0	24.8	20.0	80	33.4	5.7	27.7
2		10.6	8.5	68	31.0	11.5	19.5
3		2.11	1.7	60	33.5	16.7	16.8
4		0.8	0.64	45	40.0	28.4	11.6
5		0.33	0.26	42	43.0	31.8	11.2
1	9.0	6.0	1.8	61	31.6	15.1	16.5
2		2.3	0.70	50	32.0	20.5	11.5
3		0.5	0.15	40	42.0	32.3	9.7
4		0.45	0.14	37	42.0	33.6	8.4
5		0.35	0.10	–	42.5	42.5	0.0

$*$ Work of Adhesion

Table 24

Typical Values of K, K' and n with Reference to Equations 5 and 7 Under Section 4.6

System	K	K'	n
1. Corundum-organic phase	6×10^{-9}	1.035×10^3	0.33
2. Corundum-aqueous phase pH 9.0	6×10^{-9}	1.035×10^3	0.33
3. Corundum-aqueous phase pH 6.4, 7.4, 8.0 and 10.8	4.886×10^{-4}	2.01×10^7	1.40
4. Corundum-aqueous phase pH 4.4	3×10^{-8}	7.5×10^2	1.00
5. Rutile-organic phase (approximate values)	1.4×10^{-8}	8.05×10^2	0.45
6. Rutile-aqueous phase pH 7.0	5.44×10^{-8}	5.03×10^3	0.626
7. Rutile-aqueous phase pH 6.0 and 8.0	1.5×10^{-7}	9.7×10^3	0.889

For rutile-systems, $\Delta \gamma_{SO}$ values are 1.6 and 4.5 dynes/cm at 10^{-6} and 10^{-5} m/1 concentration. Corresponding $\Delta \gamma_{SW}$ values are 0.9 and 3.7 at pH 7.0 and 0.045 and 0.35 for both pH 6.0 and 8.0 at the respective concentrations.

Table 25

Changes in Interfacial Free Energies γ_{SO}, γ_{SW}, and γ_{WO} Cosθ (ergs/cm^2) with Reference to Their Respective Values at 10^{-7} mole/lit. Surfactant Concentration in the Aqueous Phase and the Corresponding Equilibrium Concentration in the Organic Phase.

Surfactant Concentration in the aqueous phase (mole/lit.)	$\Delta\gamma_{SO}$* pH in the aqueous phase			$\Delta\gamma_{SW}$ at pH 6.7,7.4, 8.0	$\Delta\gamma_{SO} - \Delta\gamma_{SW}$ pH in the aqueous phase			$\Delta(\gamma_{WO}$ Cosθ)**	
	6.7	7.4	8.0		6.7	7.4	8.0	pH 6.7 and 8.0	pH 7.4
10^{-7}	0	0	0	0.0	0	0	0	0.0	0.0
5×10^{-7}	18	15	1	0.03	~18	~5	~10	1.0	1.0
10^{-6}	29	26	1	0.08	~29	~5	~16	2.5	-5.0
5×10^{-6}	66	58	33	0.7	~66	~38	~36	13.0	2.0
10^{-5}	92	78	55	2.0	90	76	48	20.0	5.0
5×10^{-5}	174	148	56	18.0	156	70	78	30.0	49.0
10^{-4}	224	188	125	50.0	174	138	76	33.0	45.0

✳ Surfactant concentrations in the organic phase were taken as 5.0, 3.1 and 0.8 times concentrations in the aqueous phase at pH 6.7, 7.4 and 8.0 respectively. At concentration corresponding to 10^{-7} m/l. aqueous concentration, $\Delta\gamma_{SO}$ values are read as 26, 22 and 14 ergs/cm^2, and each one of these were normalised as zero values. $\Delta\gamma_{SO}$ and $\Delta\gamma_{SW}$ values read from Fig. 26.

✳✳ γ_{WO} = 45 ergs/cm^2 and θ = 0° at the reference point i.e. 10^{-7} m/l. surfactant concentration in the aqueous phase.